Published in final edited form as:

J Struct Biol. 2020 December 01; 212(3): 107627. doi:10.1016/j.jsb.2020.107627.

OPG-Fc treatment partially rescues low bone mass phenotype in mature *Bgn/Fmod* deficient mice but is deleterious to the young mouse skeleton

Vardit Kram[a], **Priyam Jani**[a], **Tina M. Kilts**[a], **Li Li**[a], **Emily Y. Chu**[b], **Marian F. Young**[a]

[a]Molecular Biology of Bones and Teeth Section, National Institutes of Dental and Craniofacial Research, National Institutes of Health, Department of Health and Human Services, Bethesda, MD 20892

[b]Laboratory of Oral Connective Tissue Biology, National Institute of Arthritis and Musculoskeletal and Skin Diseases, National Institutes of Health, Department of Health and Human Services, Bethesda, MD 20892

Abstract

Biglycan (Bgn) and Fibromodulin (Fmod) are small leucine rich proteoglycans (SLRPs) which are abundant in the extra-cellular matrix (ECM) of mineralized tissues. We have previously generated a Bgn/Fmod double knock-out (DKO) mouse model and found it has a 3-fold increase in osteoclastogenesis compared with Wild type (WT) controls, resulting in a markedly low bone mass (LBM) phenotype. To try and rescue/repair the LBM phenotype of Bgn/Fmod DKO mice by suppressing osteoclast formation and activity, 3- and 26-week-old Bgn/Fmod DKO mice and age/gender matched WT controls were treated with OPG-Fc for 6 weeks after which bone parameters were evaluated using DEXA, micro-computedtomographic (μCT) and serum biomarkers analyses. In the appendicular skeleton, OPG-Fc treatment improved some morphometric and geometric parameters in both the trabecular and cortical compartments in Bgn/Fmod DKO female and male mice, especially in the repair module. For many of the skeletal parameters analyzed, the Bgn/Fmod DKO mice were more responsive to the treatment than their WT controls. In addition, we found that OPG-Fc treatment was not able to prevent or ameliorate the formation of ectopic ossification, which are common lesions seen in aged joints and are one of the phenotypical hallmarks of our Bgn/Fmod DKO model. Analysis of skull bones, specifically the occipital bone, showed the treatment recovered some parameters of LBM phenotype in the craniofacial skeleton, more so in the younger rescue module. Using OPG-Fc as treatment alleviated, yet did not

Corresponding Author: Marian F. Young, PhD, Molecular Biology of Bones and Teeth Section, National Institutes of Dental and Craniofacial Research, National Institutes of Health, Bethesda, MD 20892, Tel: 301-496-8860, myoung@dir.nidcr.nih.gov.

Author contributions:

Vardit Kram: Conceptualization, Methodology, Validation, Formal analysis, Investigation, Writing - Original Draft, Review & Editing. Priyam Jani: Formal analysis, Writing - Original Draft, Review & Editing. Tina M. Kilts: Investigation. Li Li: Investigation. Emily Y. Chu: Formal analysis, Writing- Review & Editing. Marian F. Young: Conceptualization, Writing - Original Draft, Review & Editing, Visualization, Supervision

completely restore, the severe osteopenia and mineralized tissue structural abnormalities that Bgn/Fmod DKO mice suffer from.

Keywords

Proteoglycans; Biglycan; Fibromodulin; Osteoporosis; Osteoclast; Ectopic ossification; OPG-Fc; Low Bone Mass

Introduction

In vertebrates, a continuous remodeling process - the concerted and balanced action of osteoclasts (bone-resorbing cells) and osteoblasts (bone-forming cells) determines bone mass and shape. When this equilibrium is disturbed, osteoporosis, the most prevalent degenerative disease in developed countries, ensues, leading to bone loss and increased fracture risk.

Small leucine-rich proteoglycans (SLRPs) are molecules found abundantly in the extracellular matrix (ECM) of bones. They consist of a relatively small protein core of about 40–60 kDa, containing 10–12 motifs of leucine rich repeats (LRR), 20–30 amino acids long (Iozzo and Murdoch, 1996; Schaefer and Iozzo, 2008). Based on their amino-acid sequence, the difference in the spacing of the N-terminal cysteine residues and the intron-exon organization, they were divided into five subclasses (Bella et al., 2008). All the canonical SLRPs undergo post-translational modification in the form of glycosaminoglycan (GAG) chain attachments. SLRPs are structural molecules, known to regulate collagen organization (Chen et al., 2014; Kalamajski and Oldberg, 2010) but are also involved in cell signaling through the sequestration and release of ECM bound growth factors, such as BMP, TGFβ, FGFs and more (Droguett et al., 2006; Hardingham and Fosang, 1992; Hildebrand et al., 1994; Takeuchi et al., 1994; Wang et al., 2014; Winge et al., 2015; Yamaguchi et al., 1990). The direct binding of these molecules to sites on the core protein or to the GAG chains controls their bioavailability and activity, which in turn, affects cell differentiation and hard-tissue remodeling (Bi et al., 2006; Chen et al., 2004; Kram et al., 2017; Miguez et al., 2011; Mochida et al., 2006; Schaefer and Iozzo, 2008; Waddington et al., 2003). Class I SLRPs include decorin (Dcn), biglycan (Bgn), and asporin (Asp), which except for Asp, bear chondroitin sulfate or dermatan sulfate GAG side chains. Class II SLRPs include lumican (Lum) and fibromodulin (Fmod), both of which have several keratan sulfate GAG chains attached (Iozzo, 1997; Lauder et al., 1995; McEwan et al., 2006; Saamanen et al., 2001; Schaefer and Iozzo, 2008). We have previously reported that mice with double-deficiency of the 2 SLRPs, fibromodulin and biglycan (*Bgn/Fmod* DKO), acquire skeletal abnormalities including gait impairment, severe osteoarthritis and a general low bone mass phenotype (LBM), the result of enhanced osteoclast number and activity (Ameye et al., 2002; Embree et al., 2011; Kram et al., 2017; Wadhwa et al., 2005). The LBM also affected the craniofacial skeleton resulting in shorter skulls in *Bgn/Fmod* DKO mice (Kram et al., 2017).

Another hallmark of the *Bgn/Fmod* DKO mice phenotype is early onset ectopic ossification of tendons. Heterotopic or Ectopic ossification (HO/EO), is the development of mature lamellar bone at ectopic sites, mainly in soft tissues that do not normally ossify. It can either

be congenital- the result of rare genetic conditions (Fibrodysplasia ossificans progressive and Progressive osseous hyperplasia), acquired (usually caused by either trauma- fracture, blast injury, burns, surgery, or a neurogenic cause- e.g., spinal cord or central nervous system injury, stroke and brain tumors) or idiopathic, as is the case for our *Bgn/Fmod* DKO mice. The exact cellular events leading to EO are not completely elucidated, however it is thought that the pathogenesis involves inappropriate differentiation of multipotent "stem"/progenitor cells into osteoblast-and osteoclast-like cells that are not terminally differentiated (e.g. lacking osteoblast and osteoclast specific markers such as osteocalcin and cathepsin K respectively) (Al-Fakhri et al., 2005; Chalmers et al., 1975; Urist et al., 1978; Zotz et al., 2012). Histologically, EO displays as cancellous bone and mature lamellar bone, with vessels and bone marrow. These "islands" of bone are not formed within the muscle itself but rather in the connective tissue between the muscle planes (Jensen et al., 1987; Shehab et al., 2002).

Osteoclastogenesis, the recruitment and differentiation of short lived, mobile, multinucleated giant cells (100 μm in diameter) derived from the fusion of the monocytic lineage, is dependent on the expression and secretion of Receptor Activator of Nuclear Factor kappa B Ligand (RANKL) and Macrophage-Colony Stimulating Factor (M-CSF) by osteoblasts. Furthermore, the osteoblastic lineage cells also produce the decoy receptor, osteoprotegerin (OPG), an important regulator of osteoclastogenesis via its competitive inhibition of the interaction between RANKL and its receptor on the surface of preosteoclasts- RANK (Asagiri and Takayanagi, 2007; Simonet et al., 1997; Yasuda et al., 1998a; Yasuda et al., 1998b). Both RANKL and OPG are type 2 protein members of the TNFα superfamily (Locksley et al., 2001). There is a tight regulation of RANKL, OPG and M-CSF expression by cells of the osteoblastic lineage: increasing the RANKL/OPG ratio by either stimulating the expression of RANKL and/or inhibiting the production of OPG enhances osteoclastogenesis (Boyle et al., 2003). About a decade ago antiresorptive agents with a novel mechanism of action, were approved by the FDA for the treatment of osteoporosis, cancer treatment-induced bone loss, metastases to bone and giant cell tumor of bone (Belavic, 2011; Hussar and Stevenson, 2010; Kostenuik et al., 2009; Moen and Keam, 2011; Pietschmann et al., 2009). One such agent is denosumab, a fully humanized monoclonal antibody that binds with high specificity and affinity to RANKL and prevents it from activating RANK (Moen and Keam, 2011)Prolia Product Monograph, Amgen Canada Inc; 2011). This binding subsequently inhibits the recruitment, maturation and action of osteoclasts, resulting in resorption attenuation and promotion of normal bone turnover. Because denosumab only recognizes primate RANKL (Kostenuik et al., 2009), its efficacy is limited in most animal studies, therefore another RANKL inhibitor, osteoprotegerin–immunoglobulin Fc segment complex (OPG–Fc) was developed, and since then has been used in many animal studies as another means to diminish the effects of RANKL overactivation (Canon et al., 2008; Delos et al., 2008; Kim et al., 2006; Miller et al., 2007; Ominsky et al., 2007; Ominsky et al., 2008; Padagas et al., 2006).

Given that osteoclasts do not express significant levels of *Bgn* or *Fmod* (Kram et al., 2017; Li et al., 2008) and that SLRPs can regulate osteoclastogenesis via their direct interaction with M-CSF, RANKL and OPG (Ariyoshi et al., 2008; Theoleyre et al., 2006; Xaus et al., 2001), the aim of this study was to determine if OPG-Fc would ameliorate the abnormal

bone parameters of *Bgn/Fmod* DKO either by preventing the development of a LBM phenotype early in maturation or by repairing the LBM of more aged mice.

Materials and Methods

Animals

Mice deficient in both Bgn and Fmod were generated as previously described (Ameye et al., 2002). These mice were backcrossed with C57BL/6J mice (Taconic Biosciences) for 10 generations to produce *Bgn/Fmod* DKO mice on a pure C57BL/6J background. Mice were bred and kept at the NIDCR/NIH/DHHS animal facility with water and food ad libitum. All animal experiments were approved by the NIDCR/NIH/DHHS ACUC. The loss of Bgn and Fmod expression, both at the mRNA and protein levels, was confirmed by RT-PCR (genotyping), qRT-PCR and immunohistochemistry, as described previously (Kram et al., 2017).

OPG-Fc treatment

3- and 26-week-old *Bgn/Fmod* DKO mice and age/gender matched WT controls were injected S.C. with 10mg/kg OPG-Fc [Amgen] twice weekly for 6 weeks. Vehicle treated mice were subjected to the same regime but were injected with saline (vehicle control). Each experimental group had between 9 and 11 animals.

Dual-energy X-ray Absorptiometry (DEXA)

At the time of sacrifice mice were weighed and scanned with a DEXA machine (Lunar PIXImus densitometer, GE Healthcare) to determine the total bone mineral density (BMD) and total bone mineral content (BMC). When analyzing these parameters, the skulls were excluded from the region of interest.

X-ray analysis of Ectopic ossification

After dissection and fixation of the hindlimbs and vertebrae, the bones were radiographed using a Model FX-20 Faxitron X-ray system (Lincolnshire, IL, USA) at a setting of 30 kV with a 40-second exposure time and developed on Kodak X-OMAT TL films (Rochester, NY, USA), which were subsequently scanned using an Epson Expression 1680 scanner (Epson American, Inc., Long Beach, CA). The semiquantitative scoring systems used to measure the extent of ectopic ossification were previously described (Ameye et al., 2002). Briefly, a score ranging from 0 to 3 was assigned to knees and ankles independently based on the extent of ectopic radio-opaque areas observed on radiographs. A score of 0 indicated the absence of any detectable ectopic radio-opaque area. A score of 1 indicated in the knee the presence of one or two small ectopic areas and, in the ankle, a barely visible ectopic area. A score of 2 indicated in the knee three or more small ectopic radio-dense areas or the presence of a single ectopic area with a size similar to the patella and, in the ankle the occurrence of an easily visible ectopic area. A score of 3 corresponded in the knee and ankle to extensive ectopic radio-opaque areas.

Micro-computed tomography (μCT)

The skeletal phenotype of *Bgn/Fmod* DKO mice was first analyzed in whole femurs using the μCT50 system (Scanco Medical AG, Brüttisellen, Switzerland) at 70kV, 85μA, 300ms integration time and 10-μm^3 isotropic voxel size resolution. Skulls were scanned at 70kV, 85μA, 300ms integration time and 35-μm^3 resolution. Mineralized tissues were segmented by a global thresholding software. Standardized nomenclature was used for the bone parameters measured (Bouxsein et al., 2010). For the femurs, trabecular parameters were measured at the secondary spongiosa of the distal metaphysis and cortical parameters were determined in a 1mm ring at the mid-diaphyseal region according to previously published guidelines (Kohler et al., 2005). Skull scans were exported to Analyze 14.0 software (Analyzedirect, KS, USA) for further analysis. All skulls were oriented so that the transverse plane was parallel to x-axis, whereas the coronal and sagittal planes were perpendicular. Since the skull is composed of complex bone structures of varying densities, we set two different thresholds during μCT segmentation. The first threshold was set to define bone of normal density (ND) at 0.6g HA/cm^3. A second threshold defined finer bone structures of lower density (LD bone) than the rest of the skull at 0.3 to 0.59g HA/cm^3 (e.g., the squamous part of the temporal bone). In order to calculate the total volume for each skull, an elliptical shape was fabricated to encompass the skull. Mandibles and teeth were excluded from the final region of interest (ROI). The Bone Microarchitecture add-on in Analyze 14.0 was used to analyze the segmented skulls. In order to segment the occipital bone, the boundaries were first demarcated on the 3D rendering along the suture lines of occipital bone using the freehand tool in AnalyzePro. Following the demarcation of outline, the body of occipital bone was segmented manually in the sagittal sections using the freehand tool. Thresholding similar to the whole skull (ND Bone and LD Bone) was performed to look at changes in parameters specific to this bone. Five mice per group were analyzed.

Serum markers

For serum markers of bone remodeling, whole blood was collected retro-orbitally at the time of animal sacrifice. Serum was separated by centrifugation after allowing a 2-hour clotting time. Serum N-terminal propeptide of type I procollagen (PINP; cat# AC-33F1, IDS) and RatLaps™ (C-terminal telopeptides of type I collagen, CTX-I; cat# AC-06F1, IDS) were analyzed in the same specimens, with 5 biological replicates per group, using commercial EIA kits according to manufacturer's instructions.

Histology

Following μCT scanning, the femurs were embedded undecalcified in methyl methacrylate and mid-frontal longitudinal sections were prepared and stained with Von Kossa. Slides were scanned using an Aperio ScanScope (Leica Biosystems; GmbH) slide scanner.

Statistical Analysis

While skeletal parameters are known to display sexual dimorphism (Callewaert et al., 2010; Dubrow et al., 2007; Karasik and Ferrari, 2008; Laurent et al., 2014; Zanotti et al., 2014), initially all parameters were tested using a 3-way analysis of variance (ANOVA), where gender, genotype and treatment were factors. Gender was found to be a significant factor in

all and therefore we split the samples by gender and reanalyzed them as separate groups. Differences were examined by two-way ANOVA test for comparing multiple groups using either GraphPad Prism 8 or SPSS statistics V.25 (IBM; NY). Anderson-Darling test and QQ plots were used to assess normality. All data exhibited a normal distribution. Homogeneity of variances was evaluated with Levene's test, Spearman's test for heteroscedasticity, and residual plots. For heteroscedastic data, variance ratios were evaluated to determine if they would exceed limits that would compromise ANOVA robustness (Blanca et al., 2018). For data where variances were deemed unequal across groups, several steps were taken to assess validity of statistical results. Parametric and nonparametric tests were employed in parallel, resulting in comparable conclusions. To further prevent incorrect rejection of the null hypothesis, p value of <0.001 was designated as significant. Subsequently, genotype × treatment effects and main effects were assessed. Effect sizes were evaluated using partial η^2. When significant differences were indicated by ANOVA, group means were compared to determine differences between specific groups using Tukey's multiple comparisons tests. $P < 0.05$ was considered statistically significant.

Ordinal regression analysis was used on the ectopic ossification scores (SPSS statistics V.25). Five ordinal levels were assigned, data was tested for proportional odds using the test of parallel lines. Regression model was evaluated using estimates (logit regression coefficients) and standard error of the regression coefficients, which were used to calculate the Wald chi-square statistic. In some cases, the Wald chi-square statistic could not be determined because standard error was less than 0.0001, demonstrating high precision of the model. $P < 0.05$ was considered statistically significant.

Study approval

All animal studies were performed in accordance with NIH guidelines under institutionally approved protocols following the guidelines and approval of The National Institutes of Dental and Craniofacial Research Animal Care and Use Committee (protocol #18–865).

Results

Bgn/Fmod deficient (DKO) mice exhibit a markedly low bone mass (LBM) phenotype starting as early as 1 month which worsens with age (Kram et al., 2017). Here we used two approaches to test the effect OPG-Fc treatment has on bone parameters.

Prevention model:

In the prevention model, treatment was administered to skeletally immature mice starting 3 weeks after birth. At the end of the 6-week treatment period the now 9-week-old mice did not show any weight difference between treatment (OPG-Fc vs vehicle) groups in either females or males, indicating the treatment did not have an adverse effect on the animals' weight. As we reported previously, significant weight differences were found between the genotypes (WT vs DKO) [Figure 1A]. Only for the females, the interaction between treatment and genotype was also found to be significant ($F(1, 36) = 5.191$, $P=0.0287$), that is, the OPG-Fc treatment had a greater effect on the WT mice. Whole-body DEXA analysis revealed that, as expected, the OPG-Fc treatment markedly increased the BMD in both

genders (36.04% and 58.44% in treated WT and treated DKO females respectively; 41.27% and 46.81% in treated WT and treated DKO males respectively, all compared to vehicle treatment). For the females, the genotype × treatment interaction was significant with treatment and genotype exhibiting significant main effects on BMD ($F(1, 36) = 6.437$, $P=0.0157$ for interaction; $F(1, 36) = 10.58$, $P=0.0025$ for genotype and $F(1, 36) = 260.8$, $P<0.0001$ for treatment), with the treatment factor notably accounting for 83.11% of the total variation. The only two groups whose BMD did not differ significantly were the WT and DKO OPG-Fc treated (WT-O and DKO-O) groups. As for the males, both the treatment and genotype were significant factors ($F(1, 36) = 5.237$, $P=0.0281$ and $F(1, 36) = 489.9$, $P<0.0001$ for genotype and treatment respectively), but by far the differences seen were mostly due to the treatment, which accounted for over 90% of the total variation. [Figure 1B]. The same pattern was found for BMC where the treatment significantly increased the BMC in both genders (43.56% and 89.54% in treated WT and treated DKO females respectively; 62.51% and 76.13% in treated WT and treated DKO males respectively, all compared to vehicle treatment). In both genders both the genotype and treatment were associated with increased BMC, but not the interaction between them, and in both the treatment had a greater effect on the BMC than the genotype (in females $F(1, 36) = 20.02$, $P<0.0001$, partial $\eta^2=0.1172$ for genotype and $F(1, 36) = 111.5$, $P<0.0001$, partial $\eta^2=0.6529$ for treatment; in males $F(1, 37) = 6.060$, $P=0.0186$, partial $\eta^2=0.0256$ for genotype and $F(1, 37) = 189.1$, $P<0.0001$, partial $\eta^2=0.8013$ for treatment) [Figure 1C].

DEXA analysis is a fast and easy way to evaluate the animal's [total] BMD and BMC, however it is a limited technique that relies on a 2D image and stereologic models, therefore to directly measure the morphology and microarchitecture of individual bones high-resolution 3D imaging techniques are used. To determine the morphometric and geometric parameters in both the trabecular and cortical compartments of the long bone, we next analyzed the femoral bone, a murine site suitable for the assessment of both, using μCT. We have previously reported changes in the femoral length between WT and *Bgn/Fmod* DKO (Kram et al., 2017). After the treatment regimen ended, both female and male *Bgn/Fmod* DKO mice showed shorter femora compared to their WT counterparts. More interestingly, we found that in both genders, the OPG-Fc treatment also impaired the longitudinal growth of the femur. In fact, the treatment had a stronger effect than the genotype ($F(1, 34) = 27.78$, $P<0.0001$, partial $\eta^2=0.2126$ and $F(1, 34) = 63.04$, $P<0.0001$, partial $\eta^2=0.4824$ for the females' genotype and treatment respectively; $F(1, 37) = 8.568$, $P=0.0058$, partial $\eta^2=0.0778$ and $F(1, 37) = 65.16$, $P<0.0001$, partial $\eta^2=0.5919$ for the males' genotype and treatment respectively) [Figure 2A]. The changes in the trabecular BV/TV between the treated vs vehicle groups were suspiciously above our expectations (1891% and 3045% for treated WT and DKO females ; 1324% and 1406% for treated WT and DKO males, all compared to their vehicle group) [data not shown]. A closer examination revealed a mineralized mass basically filling the whole volume of the distal metaphysis of the femur [Figure 2B]. Histological examination of this area revealed a striking pathology, where most of the marrow space was occupied by acellular mineralized tissue [Figure 2C].

To evaluate the rate of remodeling in these bones, we analyzed serum markers of bone resorption (C-terminal telopeptides of type I collagen; CTX-I) and bone formation (N-terminal propeptide of type I procollagen; PINP) collected just before the mice were

sacrificed. CTX-I results showed a substantial reduction in bone resorption in the OPG-Fc treated groups in both genotypes and across both genders, but in the females only the treatment had a significant effect ($F(1, 16) = 219.1$, $P<0.0001$), accounting for 90.98% of total variation, whereas in the males, though both the interaction and the treatment itself were statistically significant factors, the treatment had a stronger effect ($F(1, 15) = 12.10$, $P=0.0034$, partial $\eta^2=0.09$ for genotype × treatment interaction vs. $F(1, 15) = 103.8$, $P<0.0001$, partial $\eta^2=0.7772$ for treatment main effect). [Figure 2D]. Surprisingly, the PINP results also showed an almost complete suppression of bone formation in the OPG-Fc treated mice, again across genotype and gender only the treatment was a significant factor ($F(1, 16) = 42.46$, $P<0.0001$ and $F(1, 16) = 41.61$, $P<0.0001$ for females and males respectively) [Figure 2E].

Another, previously reported phenotype the *Bgn/Fmod* DKO mice have is early onset EO. To assess whether the OPG-Fc treatment had any effect on the progression of this pathological process, we examined the mice's hindlimb X- rays [Figure 3A] and scored the severity of EO at two distinct locations. Ordinal regression analyses showed that in the knee, DKO female mice were 61.5 times more likely to exhibit higher EO scores compare to WTs (Wald $\chi^2(1) =9.62$, $p=0.002$). For the males, both genotype and treatment were associated with higher EO scores (Wald $\chi^2(1)=14.984$, $p<0.0001$ and Wald $\chi^2(1)=4.091$, $p=0.043$ for genotype and treatment respectively) The odds of DKO male mice to have higher scores were 119.68 times that of the WTs [Figure 3B]. Interestingly, though male DKO mice had higher EO scores compared to WT, the treatment had an opposite effect on the two genotypes- slightly lowering the scores of DKO males while increasing them in the WTs (Wald $\chi^2(1)=5.73$, $p=0.017$ for the genotype × treatment interaction).

Mineralization/ossification in the ankle seem to lag behind the knee area, as in most of the animals there were no visible radio-opaque areas present at the end of the 6-week treatment regimen. For the females, regression analyses did not apply, therefore, no conclusions regarding the effects of either genotype or treatment could be made (final model fitting $p=0.290$), however, despite not being statistically significant, there was an obvious trend pointing to higher scores in the DKO (irrespective of treatment). In the males, on the other hand, the genotype was still a predictor (Wald $\chi^2(1) =3.81$, $p=0.05$), and the odds of DKO male mice to have higher EO scores was 10.93 times that of the WTs.

Due to the marked changes in the long bones, we further looked at the skulls to determine whether the OPG-Fc treatment affected the craniofacial skeleton in a similar manner. The μCT analysis showed that in both genders, the vehicle treated *Bgn/Fmod* DKO skulls had much more low density (LD) bone (orange, Figure 4A) than the WT mice. OPG-Fc treated mice, of both genotypes, had skulls with considerably less LD bone, suggesting that the treatment converted much of the LD bone to normal density (ND) bone. In addition, we also observed some shape changes after the OPG-Fc treatment including shorter skulls and thicker zygomatic bone [data not shown]. The occipital bone was most prominently affected (Figure 4B) and we therefore analyzed the volume density parameters of this bone along with the whole skull.

Quantification of the parameters specific to occipital bone showed a significant main effect of treatment on ND volume in females ($F(1, 16) = 28.1$, $P<0.0001$, partial $\eta^2=0.637$) whereas, genotype × treatment interaction as well as both genotype and treatment as main factors were significant factors for ND bone in the males ($F(1, 16) = 13.8$, $P=0.002$, partial $\eta^2=0.462$ for genotype × treatment interaction; ($F(1, 16) = 11.6$, $P=0.004$, partial $\eta^2=0.420$ for genotype; ($F(1, 16) = 123.2$, $P<0.0001$, partial $\eta^2=0.885$ for treatment). OPG-Fc treatment significantly increased ND bone in both genotypes across both genders (28.5% in treated WT vs 44.1% in treated DKO females; 33.4% increase in treated WT vs 98.6% increase in treated DKO males; all compared to their vehicle-treated controls) (Figure 4C). LD bone volume was affected only by treatment in females ($F(1, 16) = 7.6$, $P=0.014$, partial $\eta^2=0.500$), whereas in the males both the interaction and treatment were significant ($F(1, 16) = 22.8$, $P<0.001$, partial $\eta^2=0.587$ for genotype × treatment interaction and $F(1, 16) = 23.8$, $P<0.001$, partial $\eta^2=0.598$ for treatment). Following treatment LD volume decreased significantly in female WT but not DKO mice, (−26.7% in WT vs −10.7% in DKO females), whereas in males, LD volume decreased significantly in DKO but not in WT (−0.64% vs −41.7% in WT and DKO respectively) (Figure 4D). Following treatment, the total volume of the occipital bone, with areas of both densities combined (ND and LD bone) increased significantly in both DKO females and males (28.2% and 38.9% in treated females and males respectively) (Figure 4E). The total volume, was affected only by treatment in females ($F(1, 16) = 15.9$, $P=0.001$, partial $\eta^2=0.500$), while both genotype and treatment had significant effect in males, though the effect of treatment on total volume was greater accounting for 77.5% total variance ($F(1, 16) = 55.2$, $P<0.0001$ for treatment vs $F(1, 16) = 5.1$, $P=0.039$, partial $\eta^2=0.240$ for genotype). Both genotype and treatment were found to be significant main factors affecting the density of the occipital bone in females ($F(1, 16) = 5.6$, $P=0.031$, partial $\eta^2=0.259$ for genotype and $F(1, 16) = 16.7$, $P=0.001$, partial $\eta^2=0.511$ for treatment), whereas in males the interaction between genotype and treatment as well as both main factors were significant ($F(1,16) =41.4$, $P<0.0001$, partial $\eta^2=0.721$ for genotype ×treatment interaction; $F(1, 16) = 9.4$, $P=0.007$, partial $\eta^2=0.370$ for genotype and $F(1, 16) = 142.8$, $P<0.0001$, partial $\eta^2=0.899$ for treatment). Bone density increased significantly more in the treated DKO males (7.4% and 20.1% in treated WT and DKO respectively) (Figure 4F). Whole skull was analyzed by segmenting the skull (omitting the mandible and teeth) using thresholding analogous to the occipital bone. Quantification of the μCT data for the skull as a whole revealed a similar trend (Supplementary Figure 1):ND bone volume was significantly increased after treatment in the DKO groups across gender (in females 8.0% vs. 26.7% increase in treated WT and DKO respectively; in males 8.5% increase in treated WT vs. 40.5% increase in treated DKO male mice respectively) all compared to their vehicle treated controls) (S. Fig. 1A). Correspondingly, the volume of LD bone decreased following OPG-FC treatment (S. Fig. 1B) (In females −14.0% and −11.6% in treated WT and DKO respectively; in males −10.5% vs. −15.9% in treated WT and DKO respectively). Only the treatment as main factor in females was found to be significant ($F(1,16) = 5.6$, $P=0.031$, partial $\eta^2=0.259$).

In order to normalize these findings to the skull size, we calculated the ratio of the bone volume (ND bone +LD bone) to the total volume (S. Fig. 1C). In the females, the BV/TV ratio was significantly influenced by the interaction and genotype as main factor ($F(1,16)$

=10.4, P=0.005, partial η^2=0.395 for interaction; F (1,16) =4.6, P=0.048, partial η^2=0.222 for genotype). In the males, though both genotype and treatment were found to be significant in influencing the BV/TV, the genotype had a stronger effect on this parameter accounting for 49.7% of total variance((F (1,16) =4.6, P=0.001, partial η^2=0. for genotype and F (1,16) =2.7, P=0.007, partial η^2=0.369 for treatment). Across both genders, treatment was the only factor influencing BMD showed significant difference with treatment in both genders (F (1,16) =6.2, P=0.024, partial η2=0.280 in females and F (1,16) =19.4, P<0.0001 partial η2=0.548 in males) (S. Fig 1D).

In summary, OPG-Fc treatment caused drastic changes in the skull as a whole with marked changes in the density. The changes in volume resulted in generalized thickening of the occipital bone (data not shown). The *Bgn/Fmod* DKO mice skulls were more affected by treatment than WT mice. Also, males showed more pronounced changes than females.

Repair model:

for this model we let the "natural" course of aging as well as the full *Bgn/Fmod* DKO phenotype to develop and tried to evaluate whether OPG-Fc treatment can rescue, at least to some extent, the damage that was already found in the skeleton. At the end of the treatment regimen, the animals were 32 weeks old. For both females and males, only the genotype was a significant factor in influencing the whole-body weight accounting for 11.96% of variance in females (F (1, 36) = 5.409, P=0.0258) and 43.86% of the variance in males (F (1, 35) = 29.17 , P<0.0001) [Figure 5A]. Though in females and males, both the genotype and the treatment were significant main factors influencing BMD in both genders, the treatment had a greater effect than the genotype (F (1, 36) = 8.637, P=0.0057, partial η^2=0.2959 for genotype and F (1, 36) = 19.41, P<0.0001, partial η^2=0.1316 for treatment in females; F (1, 34) = 9.303, P=0.0044, partial η^2=0.222 for genotype and F (1, 34) = 13.19, P=0.0009, partial η^2=0.1566 for treatment in males). Across both genders, the treatment had a (not statistically significant) bigger effect on the DKO mice (5.7% increase in treated WT vs. 11.03% in treated DKO females; 2.8% increase vs. 12.19% increase in treated WT and DKO males respectively, all compared to their vehicle controls), rendering the BMD of the OPG-Fc treated mice comparable to that of the "naïve" WTs, thus basically restoring this parameter[Figure 5B].In terms of BMC, though both the treatment and genotype were significant main factors associated with increased BMC in females, the effect of the genotype was larger accounting for 24.13% of the variance (F (1, 36) = 14.37, P=0.0006 for genotype vs. F (1, 36) = 6.566, P=0.0147, partial η^2=0.1102 for treatment). In the males, on the other hand, only the genotype significantly influenced BMC, accounting for over 33% of the variance (F (1, 35) = 19.78, P<0.0001). As with the BMD, though not statistically significant, in both genders it seemed that the OPG-Fc treatment had a stronger effect on the DKO mice (2.76% increase in treated WT vs. 14.54% increase in treated DKO females; 1.30% increase in treated WT vs. 23.70% increase in treated DKO males, all compared to their vehicle controls), again comparing the BMC of DKO-O mice to that of WT-V ones [Figure 5C]. Thus, to summarize, DEXA analysis indicated, that in both females and males, the OPG-Fc treatment resulted in an increase of both BMD and BMC and was able to restore the defect the DKO mice suffer from.

Since the growth plates of murine long bones do not close, there is continuous longitudinal growth even at advanced age. The differences seen in the femoral length were only determined by the genotype of mice, ($F(1, 36) = 34.58$, $P<0.0001$, partial $\eta^2=0.49$; $F(1, 35) = 121.8$, $P<0.0001$, partial $\eta^2=0.777$ for females and males respectively) [Figures 6A–B]. Examination of the trabecular compartment revealed the OPG-Fc treatment was able to increase the BV/TV in both genders and for both genotypes. In fact, in the females the treatment and genotype had similar contributions to the BV/TV ($F(1, 36) = 35.67$, $P<0.0001$, partial $\eta^2=0.3356$ for genotype and $F(1, 36) = 32.58$, $P<0.0001$, partial $\eta^2=0.3066$ for treatment), whereas in the males the genotype × treatment interaction, as well as genotype and treatment as main effect were significant, though by far the genotype had the strongest effect ($F(1, 34) = 4.168$, $P=0.0490$, partial $\eta^2=0.0232$ for interaction; $F(1, 34) = 108.0$, $P<0.0001$, partial $\eta^2=0.6036$ for genotype and $F(1, 34) = 33.93$, $P<0.0001$, partial $\eta^2=0.1896$ for treatment)). Again, for both females and males, the OPG-Fc treatment was more effective in increasing the BV/TV in the DKO groups (112.47% increase in treated WT vs. 237.73% increase in treated DKO females; 63.58% increase in treated WT vs. 158.78% in treated DKO male mice, all compared to their vehicle controls) [Figure 6C&D].

For the trabecular number, in both females and males, though both the genotype and treatment were significant main factors, the genotype had a stronger effect than the treatment ($F(1, 36) = 57.71$, $P<0.0001$, partial $\eta^2=0.5616$ for genotype vs. $F(1, 36) = 7.521$, $P=0.0094$, partial $\eta^2=0.0732$ for treatment in females and $F(1, 35) = 61.66$, $P<0.0001$, partial $\eta^2=0.4845$ for genotype and $F(1, 35) = 28.12$, $P<0.0001$, partial $\eta^2=0.221$ for treatment in males). Surprisingly, the DKO females were effected to a lesser degree than the WT by the OPG-Fc treatment, while in the males the increase in trabecular number after OPG-Fc treatment was more noticeable in the DKO group (15.01% vs. 7.53% in treated WT and DKO females respectively; 24.89% and 33.03% for treated WT and DKO males respectively, all compared to their vehicle treated controls). [Figure 7A]. In the females, only the treatment was a significant factor affecting trabecular thickness, accounting for 22.62% of the total variance ($F(1, 36) = 11.13$, $P=0.0020$), whereas for the males, both genotype and treatment were significant main factors influencing the thickness ($F(1, 34) = 14.30$, $P=0.0006$, partial $\eta^2=0.2487$; $F(1, 34) = 7.929$, $P=0.0080$, partial $\eta^2=0.1379$). [Figure 7B]. The spacing between the trabeculae is a corollary of both the number and thickness, therefore it was not surprising to find significant differences between the groups across both genders. In both females and males, though both the genotype and treatment were significant main factors, the genotype was a more influential factor, accounting for over 53% of the total variation in both genders (In females $F(1, 34) = 50.59$, $P<0.0001$, partial $\eta^2=0.5465$ for genotype and $F(1, 34) = 7.583$, $P=0.0094$, partial $\eta^2=0.0819$ for treatment; In males $F(1, 34) = 64.58$, $P<0.0001$, partial $\eta^2=0.5308$ for genotype and $F(1, 34) = 22.98$, $P<0.0001$, partial $\eta^2=0.1889$ for treatment). Taken together, these data indicate that in the females the overall increase in the BV/TV was due more to an increase in the thickness of existing trabeculae than formation of new trabeculae (15.01% and 7.53% increase in Tb. N. in treated WT and DKO mice compared to 34.96% and 22.21% increase in Tb. Th. in treated WT and DKO mice), whereas in the males the treatment increased the number of trabeculae more than their thickness (24.89% and 33.03% increase in Tb. vs. 10.01% and 24.16% increase in Tb. Th. in treated WT and DKO mice). [Figure 7C]. The connectivity density, a parameter

describing the architectural integrity of the trabecular network, was affected by both the genotype and the treatment in both females and males ($F(1, 34) = 20.25$, $P<0.0001$, partial $\eta^2=0.2411$ for genotype vs. $F(1, 34) = 24.07$, $P<0.0001$, partial $\eta^2=0.2867$ for treatment in females; $F(1, 35) = 64.40$, $P<0.0001$, partial $\eta^2=0.5578$ for genotype vs. $F(1, 35) = 11.36$, $P=0.0018$, partial $\eta^2=0.0983$ for treatment in males). [Figure 7D].

Since the cortical and trabecular bone compartments are subject to different regulatory mechanisms, we also wanted to assess the efficacy of the OPG-Fc treatment on cortical parameters. Cortical thickness was differently affected in females and males. For the females, only the genotype was a significant factor, accounting for 25.08% of total variation ($F(1, 36) = 13.45$, $P=0.0008$). Whereby even before the treatment, the *Bgn/Fmod* DKO mice displayed somewhat thicker cortices, at the end of the 6- week treatment course this parameter did not change significantly (3.02% vs. 7.79% increase for treated WT and treated DKO respectively, compared to vehicle treated mice). In the males on the other hand, both the genotype and treatment had a significant effect on the cortical thickness, but the genotype had a stronger influence ($F(1, 35) = 100.6$, $P<0.0001$, partial $\eta^2=0.6477$ for genotype vs. $F(1, 35) = 21.01$, $P<0.0001$, partial $\eta^2=0.1353$ for treatment). Here also, the DKO mice had thicker cortices to begin with and in both genotypes the OPG-Fc treatment resulted in thickening of the cortex, though to a greater degree in the WT (16.42% vs. 6.56% increase in treated -WT and -DKO, respectively, compared to their vehicle controls) [Figure 8A]. Though the DKO female mice started with narrower diaphyses compared to their WT counterparts, the OPG-Fc treatment increased this parameter beyond the value of the treated WTs, thus it was not surprising to find both the treatment and the genotype × treatment interaction as significant factors affecting this index ($F(1, 35) = 6.429$, $P=0.0159$, partial $\eta^2=0.1182$ for genotype × treatment interaction and $F(1, 35) = 13.38$, $P=0.0008$, partial $\eta^2=0.2461$ for treatment). For the males, both the genotype and the treatment were significant effectors ($F(1, 35) = 6.441$, $P=0.0158$, partial $\eta^2=0.1334$ and $F(1, 35) = 6.080$, $P=0.0187$, partial $\eta^2=0.1259$for genotype and treatment respectively) [Figure 8B]. In both genders, the *Bgn/Fmod* DKO mice started out with narrower medullary diameters and the treatment had opposite effects on WT and DKO mice; the OPG-Fc treated WT showed a mild reduction in the diameter, whereas the DKO mice treated with OPG-Fc showed an increase in this parameter (−0.56% vs. 3.48% in treated WT and treated DKO females respectively; −13.18% vs. 2.91% in treated WT and treated DKO males respectively, all compared to their respective vehicle controls). In the females, only the genotype was found to significantly influence medullary cavity diameter, accounting for 38.79% of the total variance ($F(1, 36) = 24.25$, $P<0.0001$), whereas for the males the interaction as well as both individual main factors significantly influenced the observed variance ($F(1, 33) = 14.58$, $P=0.0006$, partial $\eta^2=0.102$; $F(1, 33) = 82.91$, $P<0.0001$, partial $\eta^2=0.58$ and $F(1, 33) = 15.23$, $P=0.0004$, partial $\eta^2=0.1065$ for genotype × treatment interaction, genotype and treatment respectively) [Figure 8C]. Taken together, these results indicate that in both WT and DKO females and the DKO males the cortical thickening in the treated mice was due to periosteal apposition of new bone. In the WT males, on the other hand, it seems there was both endosteal and periosteal apposition of new bone.

Looking at the serum markers for bone resorption revealed that, as expected, OPG-Fc treatment lowered the levels of CTX-I. Though in both females and males, the DKO mice

start at a lower serum level of CTX-I than the WTs, only the treatment was found to be a significant main effect accounting for over 30% of the total variance (F (1, 16) = 8.770, P=0.0092, partial η^2=0.3077 and F (1, 16) = 12.61, P=0.0027, partial η^2=0.3863 for females and males respectively).Therefore, the effect of OPG-Fc treatment was more marked in the WT (−53.84% vs. −20.18% in treated -WT and -DKO females respectively; −41.09% vs. −16.60% in treated -WT and -DKO male mice respectively, all compared to their vehicle controls) [Figure 8D]. As with the young mice, the OPG-Fc treatment also lowered the levels of PINP in the mouse serum. Once more, because in both females and males the DKO mice had a lower baseline level, the treatment had a stronger effect on the WTs (−66.40% vs. −53.33% reduction in PINP levels in treated WT and treated DKO females respectively; −70.67% vs. −4.69% reduction in PINP levels in treated WT and treated DKO males respectively, compared to vehicle controls). For the females, only the treatment was a significant factor, accounting for 69.85% of the total variance(F (1, 16) = 44.75, P<0.0001), while for the males the interaction between genotype and treatment as well as both the genotype and treatment as main factors all had a significant influence on the PINP serum level (F (1, 16) = 13.68, P=0.0019, partial η^2=0.2581 for genotype × treatment interaction; F (1, 16) = 8.149, P=0.0115, partial η^2=0.1538 for genotype main factor and F (1, 16) = 15.17, P=0.0013, partial η^2=0.28.62 for treatment as main factor)[Figure 8E].

As ectopic ossification is a pathological process that worsens with age, we were curious to see whether the OPG-Fc treatment influenced its progression. Examination of the hindlimb x-rays indicated that compared to the young mice (in the prevention module), there were more and broader areas of ectopic ossifications in both WT and DKO mice across both genders [Figure 9A]. Scoring the two distinct sites- the knee and ankle- revealed that again, the DKO mice tended to have higher scores compared to their WT counterparts, the result of both more and larger radio opaque areas. For both locations and in both genders, only genotype was found to have an effect on the amount and/or size of the ectopic ossification whereas the OPG-Fc treatment was not effective in either ameliorating nor exacerbating the progression of this pathology (For females: Wald χ^2(1)= 4.904, p<0.000 ; Wald χ^2(1)=12.697, p=0.000 for genotype in the knee and ankle respectively. For males: Wald χ^2(1) =319.659, p=0.000 and Wald χ^2(1) =189.314p=0.000 for genotype in the knee and ankle respectively), making the odds of DKO mice (females and males) having more/bigger EO lesions in their knees at least a 100 times that of WTs and more than 50 times that of WTs in the ankle [Figure 9B&C].

μCT analysis of the skulls showed that, unlike the young mice, OPG-Fc treatment did not completely rescue the low density phenotype in skulls of older mice (Figure 10A). Similar to the young mice, in the older mice of the repair module, males had more changes in the occipital bone parameters than females (Figure 10B). OPG-Fc treatment increased the ND volume (Figure 10C), total volume (Figure 10E) and bone density (Figure 10F) in females and males, but the changes were not statistically significant. In terms of LD volume (Figure 10D), no differences were found between any of the experimental groups in females, whereas in the males, genotype had a significant influence on LD volume explaining 36.9% of the total variance (F (1,15) = 7.8, P=0.016). In females, OPG-Fc treatment was a significant factor influencing the total volume (F (1,15) = 4.7, P=0.046, partial η^2 = 0.239). No interaction or main factors significantly affected this parameter in male mice (Figure

10E). In both females and males, only the genotype had a significant effect on the bone density ($F(1,15) = 25.2$, $P<0.001$, partial $\eta^2 = 0.627$ for females and $F(1,15) = 8.7$, $P=0.011$, partial $\eta^2 = 0.401$ for males respectively) (Figure 10F). In the whole skull analysis (Supplementary Figure 2), only the DKO males exhibited significant increase in ND bone volume ($F(1,14) = 580.8$, $P<0.001$, partial $\eta2 = 0.620$) and BV/TV ($F(1,14) = 17.2$, $P=0.001$, partial $\eta^2 = 0.552$) . OPG-Fc treatment had a positive effect on BMD. For females and males alike both genotype and treatment were found to be significant factors (In females: ($F(1,15) = 27.1$, $P<0.001$, partial $\eta^2 = 0.643$ for genotype and $F(1,15) = 7.1$, $P=0.018$, partial $\eta2 = 0.321$; In males: $F(1,14) = 37.6$, $P<0.0001$, partial $\eta2 = 0.729$ for genotype and ($F(1,14) = 22.9$, $P<0.001$, partial $\eta2 = 0.620$ for treatment).

This data shows that OPG-Fc treatment does not affect the adult skulls as drastically as the skulls in younger mice. However, the milder changes in volume and density indicate that bone remodeling process in adult mice is affected to some extent by OPG-Fc treatment regardless of the genotype.

Discussion

Proteoglycans in general, and SLRPs specifically, are known to play a crucial role in skeletal health. We and others have previously shown skeletal defects in mouse models lacking one or more of these ECM proteoglycans (Ameye and Young, 2002; Bi et al., 2006; Boskey et al., 2005; Corsi et al., 2002; Goldberg et al., 2006; Xu et al., 1998). Our *Bgn/Fmod* double deficient mouse model exhibits an upsurge in osteoclastogenesis resulting in profound low bone mass (LBM) phenotype that is already significant at 5 weeks of age, yet still worsens with age (Kram et al., 2017). In recent years, denosumab, a fully human monoclonal immunoglobulin G2 antibody against RANKL has been approved for treatment of various pathological conditions in which the etiology is increased osteoclast activity (Cummings et al., 2009; Kostenuik et al., 2009). Denosumab's advantage is that, unlike conventional bisphosphonates, it is not incorporated into the bone matrix, which initially deemed it suitable for long-term therapy and use in children (Baron et al., 2011; Boyce, 2017; Brown et al., 2009; Ellis et al., 2008). Because denosumab only recognizes primate RANKL, OPG- and soluble RANK-immunoglobulin Fc segment complexes were developed to inhibit osteoclast formation and activity in preclinical animal models (Canon et al., 2008; Delos et al., 2008; Ominsky et al., 2008; Padagas et al., 2006).

The purpose of this study was to assess whether OPG-Fc treatment could either prevent the LBM in the *Bgn/Fmod* DKO from developing or cure it once it is already established. We followed the provider's recommended dosage of 10mg/kg twice a week for 6 weeks with either 3- or 26-week old mice and evaluated their skeletal parameters at the endpoint. With regard to the axial skeleton, in the prevention arm of the experiment, it initially seemed like the treatment was effective: across both genders and genotypes, the treated groups showed a noticeable increase in both BMD and BMC as measured by DEXA; However, on closer examination, a pathological phenotype was revealed, where the metaphyses were completely calcified/mineralized (though we did not investigate this further to be able to discern) with practically all of the marrow space obliterated. This is reminiscent of the congenital form of osteopetrosis. Due to this interruption to the primary spongiosa, all treated groups showed a

marked growth inhibition indicated by the shortened femoral length. Moreover, our results indicate that OPG-Fc treatment significantly reduced serum biochemical markers of both bone resorption and formation. Though some inhibition of bone formation markers is expected with antiresorptive treatments (Reid et al., 2010; Sipos et al., 2011), since there are no active osteoclast resorbing bone, and hence no recruitment of newly differentiated osteoblasts to fill out resorptive pits, a complete arrest of the remodeling process was not expected given these were young mice at the peak of their growth period. Our results resemble findings of other groups using different treatment protocols (dosage, duration, species] of OPG-Fc in young/juvenile subjects (Bargman et al., 2012; Ominsky et al., 2007; Reid et al., 2010; Sipos et al., 2011). In fact, Sipos et al. showed 40–70% reduction in serum bone markers as early as 5 days after initiating the OPG-FC treatment (Sipos et al., 2011) and Bargman et al. showed adverse reaction of the young (mouse) skeleton even with low dose OPG-Fc treatment (1 mg/kg/week for 4 weeks) (Bargman et al., 2012).

The effect of OPG-Fc treatment on mature/old mice (past the rapid bone accrual stage) is quite different as the rescue arm of the present study indicates. As with the young mice, DEXA analysis showed a substantial increase in both the BMD and BMC indices in the treated groups across both genders and genotypes. It is important to note that the treatment had a greater effect on the *Bgn/Fmod* DKO mice compared to the WTs, probably because their starting point is much lower. The μCT results revealed improvement of specific bone architectural parameters induced by the OPG-Fc-treatment, some of which were actually restored to the level of the naïve WTs. Though the murine skeleton undergoes continuous elongation, the rate at which this longitudinal growth happens is much slower as the animal ages. Therefore, it was not surprising to not find significant differences between OPG-Fc- and vehicle-treated mice after only 6 weeks of treatment, and having the genotype be a significant factor to femur length. OPG-Fc treatment led to higher trabecular BV/TV and improved trabecular architecture. In the females, increases in both trabecular number and thickness were seen in the WT treated group, whereas the *Bgn/Fmod* DKO females only exhibited a significant change in the thickness parameter as a result of the treatment. For the males, the elevated BV/TV was mostly the result of increased trabecular number and not thickness in both *Bgn/Fmod* DKO and their WT controls. The connectivity density, a measurement of the architectural integrity of the trabecular bone, was also improved by the OPG-Fc treatment in both females and males. Likewise, the cortical bone was affected by the treatment, as all treated groups across both genders displayed an increase in cortical thickness (though not always a statistically significant one). In both females and males, the variances seen between groups in most parameters was due to genotype rather than the treatment factor, though at least in some indices treatment was a significant factor. Moreover, an interaction between genotype and treatment was also found in some of the parameters analyzed, indicating the two genotypes responded to the treatment differently (sometimes the magnitude of the effect was different in others the response was opposite). Taken together, these results indicate that OPG-Fc treatment in mature mice can improve many of the impaired skeletal indices of the *Bgn/Fmod* DKO mice, though even with the treatment, most of the skeletal indices were not restored to the level of the untreated WTs. The analysis of serum markers again revealed that both resorption as well as formation were affected by the treatment. Despite both biochemical indicators being reduced in OPG-Fc-vs.

vehicle-treated mice, we believe that because in both females and males the *Bgn/Fmod* DKO mice had a lower baseline level, the treatment had a stronger effect on the WT mice. It is interesting to note that DKO-V mice have lower serum levels of CTX-I compared to their age matched controls. This corresponds to the fewer Osc/Tb. Perimeter we reported in older *Bgn/Fmod* DKO mice. We hypothesized the enhanced osteoclastogenesis at a young age resulted in such low bone perimeter/surface, that there was very little (if any) resorption going on (Kram et al., 2017).

The craniofacial skeleton differs developmentally and structurally from the appendicular skeleton (Chai and Maxson Jr, 2006; Wilkie and Morriss-Kay, 2001) and in this study we show it also reacted differently to the OPG-Fc treatment. Although not as debilitating as the long bone, OPG-Fc treatment drastically affected the skull bones in the young group. In the young mice, though the treatment managed to improve some of the skulls' parameters, there are also some side effects in the form of morphological changes that still need further investigation. The moderate changes in adult mice due to OPG-Fc treatment shows that despite having completed growth, the remodeling bone is still sensitive to OPG. The skull bones also differ in their developmental origin and future studies warrant investigation on how different bones could be affected.

The early onset EO seen in our *Bgn/Fmod* DKO mouse model is idiopathic. In such cases proximal joints are typically more involved (e.g. knee vs. ankle) and often the lesions are seen in more than a single region (Edwards and Clasper, 2015; Shehab et al., 2002). Though in many cases, early EO formation is subclinical and only noted on radiographs, prophylaxis and/or early treatment of EO is extremely important to prevent progression and complications, which in severe cases may include debilitating pain, peripheral nerve entrapment and restricted range of motion up to ankylosis and full loss of joint mobility (Shehab et al., 2002). EO has repeatedly been shown to be an inflammatory related process, with cytokines such as TNFα being involved (Shehab et al., 2002), therefore, nonsteroidal anti-inflammatory drugs may be used for therapy. Moreover, demineralized bone matrix (as a result of inflammation or trauma) can also invoke EO, by releasing osteogenic growth factors and cytokines such as BMPs (Shehab et al., 2002; Urist et al., 1978).

Interestingly, decorin, aggrecan and biglycan were all detected in ectopic bone but in lower amounts compared to normal bone, and differences in proteoglycan concentrations in heterotopic bone samples may reflect different pathophysiology and development patterns (Mania et al., 2009).

PGs play a role in the mineralization process of bone, largely by controlling the availability of growth factors and cytokines. In our *Bgn/Fmod* DKO model (Kram et al., 2017), the lack of these two SLRPs results in increased TNFα activity, and hence increased osteoclastogenesis, as well as inflammatory potential, which may explain the amplified EO phenotype in the *Bgn/Fmod* DKO compared to WT controls (earlier onset, more and bigger lesions). The elevated TNFα signaling in the *Bgn/Fmod* DKO mice might also explain why the OPG-Fc treatment, though obviously eradicating osteoclast activity, did not influence the EO state. Our *Bgn/Fmod* DKO model has been shown to have restricted range of joint

motion (Ameye et al., 2002), though initially attributed to abnormal collagen fibrils in tendons it could also be the result of the extensive EO lesions, especially at an advanced age.

In the mature mice, the OPG-Fc treatment protocol we implemented clearly resulted in improvement of specific bone architectural parameters, some of which were restored to the level of the naive WTs, but based on the serum markers, it also affected the formation stage of the remodeling cycle (most probably elongating this phase). Though the reversible nature of OPG-Fc or denosumab treatment is well established (Bargman et al., 2012; Bekker et al., 2004; Boyce, 2017; Iranikhah et al., 2018; Kim et al., 2006; Kostenuik et al., 2009), our and others results point to a deleterious effect of OPG-Fc treatment on the “pediatric” skeleton. Consequently, more research needs to be done on the young, pre-puberty population. Clinically, the benefits of such antiresorptive treatment must seriously outweigh the risks and/or side-effects (e.g., growth arrest, obliteration of marrow space).

In summary, we find that LBM phenotype in the *Bgn/Fmod* DKO model could be partially rescued by OPG-Fc treatment in mature mice, but in young mice, even though effective in enhancing BMD, treatment was harmful to the skeletal structure independent of genotype. While overactive osteoclastogenesis in the *Bgn/Fmod* DKO model appeared to be reduced by the OPG-Fc and somewhat beneficial to the mineralized tissue, the nature, quality and strength of the new bone produced is not known. Further experiments will be needed to determine if additional factors could be used to achieve full effectiveness of OPG-Fc in cases of ECM disruption caused by loss of *Bgn/Fmod*.

Supplementary Material

Refer to Web version on PubMed Central for supplementary material.

Acknowledgments

The research was supported in part by the Intramural Research Program of the NIH, NIDCR Molecular Biology of Bones and Teeth Section (Z01DE000379-35) and the Veterinary Resources Core (ZICDE000740-05). We would like to thank Amgen, who generously provided the OPG-fc used in the investigation (CRADA T-2011-1587). We also thank Dr. Kristen Pan for advising on statistical matters.

Abbreviations:

Bgn	Biglycan
Fmod	Fibromodulin
DKO	Double knockout
LBM	Low bone Mass
OPG-Fc	Osteoprotegerin– immunoglobulin Fc segment complex
ECM	Extracellular Matrix
SLRPs	Small Leucine-rich Proteoglycans
GAG	Glycosaminoglycans

RANKL	Receptor Activator of Nuclear Factor κ B Ligand
DEXA	Dual-energy X-ray Absorptiometry
μCT	Micro-computed tomography
BMD	Bone Mineral Density
BMC	Bone Mineral Content
BV/TV	Bone volume to total volume ratio

References:

Al-Fakhri N, Hofbauer LC, Preissner KT, Franke FE, Schoppet M, 2005 Expression of bone-regulating factors osteoprotegerin (OPG) and receptor activator of NF-kappaB ligand (RANKL) in heterotopic vascular ossification. Thromb Haemost 94, 1335–1337. [PubMed: 16411417]

Ameye L, Young MF, 2002 Mice deficient in small leucine-rich proteoglycans: novel in vivo models for osteoporosis, osteoarthritis, Ehlers-Danlos syndrome, muscular dystrophy, and corneal diseases. Glycobiology 12, 107R–116R.

Ameye L, Aria D, Jepsen K, Oldberg A, Xu T, Young MF, 2002 Abnormal collagen fibrils in tendons of biglycan/fibromodulin-deficient mice lead to gait impairment, ectopic ossification, and osteoarthritis. FASEB J. 16, 673–680. [PubMed: 11978731]

Ariyoshi W, Takahashi T, Kanno T, Ichimiya H, Shinmyouzu K, Takano H, Koseki T, Nishihara T, 2008 Heparin inhibits osteoclastic differentiation and function. J Cell Biochem 103, 1707–1717. [PubMed: 18231993]

Asagiri M, Takayanagi H, 2007 The molecular understanding of osteoclast differentiation. Bone 40, 251–264. [PubMed: 17098490]

Bargman R, Posham R, Boskey A, Carter E, DiCarlo E, Verdelis K, Raggio C, Pleshko N, 2012 High- and low-dose OPG-Fc cause osteopetrosis-like changes in infant mice. Pediatr. Res 72, 495–501. [PubMed: 22926546]

Baron R, Ferrari S, Russell RG, 2011 Denosumab and bisphosphonates: different mechanisms of action and effects. Bone 48, 677–692. [PubMed: 21145999]

Bekker PJ, Holloway DL, Rasmussen AS, Murphy R, Martin SW, Leese PT, Holmes GB, Dunstan CR, DePaoli AM, 2004 A single-dose placebo-controlled study of AMG 162, a fully human monoclonal antibody to RANKL, in postmenopausal women. J Bone Miner Res 19, 1059–1066. [PubMed: 15176987]

Belavic JM, 2011 Denosumab (Prolia): A new option in the treatment of osteoporosis. Nurse Pract 36, 11–12.

Bella J, Hindle KL, McEwan PA, Lovell SC, 2008 The leucine-rich repeat structure. Cell Mol Life Sci 65, 2307–2333. [PubMed: 18408889]

Bi Y, Nielsen KL, Kilts TM, Yoon A, M AK, Wimer HF, Greenfield EM, Heegaard AM, Young MF, 2006 Biglycan deficiency increases osteoclast differentiation and activity due to defective osteoblasts. Bone 38, 778–786. [PubMed: 16364709]

Blanca MJ, Alarcón R, Arnau J, Bono R, Bendayan R, 2018 Effect of variance ratio on ANOVA robustness: Might 1.5 be the limit? Behav. Res. Methods 50, 937–962. [PubMed: 28643157]

Boskey AL, Young MF, Kilts T, Verdelis K, 2005 Variation in mineral properties in normal and mutant bones and teeth. Cells Tissues Organs 181, 144–153. [PubMed: 16612080]

Bouxsein ML, Boyd SK, Christiansen BA, Guldberg RE, Jepsen KJ, Müller R, 2010 Guidelines for assessment of bone microstructure in rodents using micro-computed tomography. J Bone Miner Res 25, 1468–1486. [PubMed: 20533309]

Boyce AM, 2017 Denosumab: an Emerging Therapy in Pediatric Bone Disorders. Curr Osteoporos Rep 15, 283–292. [PubMed: 28643220]

Boyle WJ, Simonet WS, Lacey DL, 2003 Osteoclast differentiation and activation. Nature 423, 337–342. [PubMed: 12748652]

Brown JP, Prince RL, Deal C, Recker RR, Kiel DP, de Gregorio LH, Hadji P, Hofbauer LC, Alvaro-Gracia JM, Wang H, Austin M, Wagman RB, Newmark R, Libanati C, San Martin J, Bone HG, 2009 Comparison of the effect of denosumab and alendronate on BMD and biochemical markers of bone turnover in postmenopausal women with low bone mass: a randomized, blinded, phase 3 trial. J Bone Miner Res 24, 153–161. [PubMed: 18767928]

Callewaert F, Sinnesael M, Gielen E, Boonen S, Vanderschueren D, 2010 Skeletal sexual dimorphism: relative contribution of sex steroids, GH-IGF1, and mechanical loading. J Endocrinol 207, 127–134. [PubMed: 20807726]

Canon JR, Roudier M, Bryant R, Morony S, Stolina M, Kostenuik PJ, Dougall WC, 2008 Inhibition of RANKL blocks skeletal tumor progression and improves survival in a mouse model of breast cancer bone metastasis. Clin Exp Metastasis 25, 119–129. [PubMed: 18064531]

Chai Y, Maxson RE Jr, 2006 Recent advances in craniofacial morphogenesis. Dev. Dyn 235, 2353–2375. [PubMed: 16680722]

Chalmers J, Gray DH, Rush J, 1975 Observations on the induction of bone in soft tissues. J Bone Joint Surg Br 57, 36–45. [PubMed: 1090627]

Chen S, Young MF, Chakravarti S, Birk DE, 2014 Interclass small leucine-rich repeat proteoglycan interactions regulate collagen fibrillogenesis and corneal stromal assembly. Matrix Biol 35, 103–111. [PubMed: 24447998]

Chen XD, Fisher LW, Robey PG, Young MF, 2004 The small leucine-rich proteoglycan biglycan modulates BMP-4-induced osteoblast differentiation. FASEB J 18, 948–958. [PubMed: 15173106]

Corsi A, Xu T, Chen XD, Boyde A, Liang J, Mankani M, Sommer B, Iozzo RV, Eichstetter I, Robey PG, Bianco P, Young MF, 2002 Phenotypic effects of biglycan deficiency are linked to collagen fibril abnormalities, are synergized by decorin deficiency, and mimic Ehlers-Danlos-like changes in bone and other connective tissues. J Bone Miner Res 17, 1180–1189. [PubMed: 12102052]

Cummings SR, San Martin J, McClung MR, Siris ES, Eastell R, Reid IR, Delmas P, Zoog HB, Austin M, Wang A, Kutilek S, Adami S, Zanchetta J, Libanati C, Siddhanti S, Christiansen C, Trial F, 2009 Denosumab for prevention of fractures in postmenopausal women with osteoporosis. N Engl J Med 361, 756–765. [PubMed: 19671655]

Delos D, Yang X, Ricciardi BF, Myers ER, Bostrom MP, Camacho NP, 2008 The effects of RANKL inhibition on fracture healing and bone strength in a mouse model of osteogenesis imperfecta. J Orthop Res 26, 153–164. [PubMed: 17729310]

Droguett R, Cabello-Verrugio C, Riquelme C, Brandan E, 2006 Extracellular proteoglycans modify TGF-beta bio-availability attenuating its signaling during skeletal muscle differentiation. Matrix Biol 25, 332–341. [PubMed: 16766169]

Dubrow SA, Hruby PM, Akhter MP, 2007 Gender specific LRP5 influences on trabecular bone structure and strength. J Musculoskelet Neuronal Interact 7, 166–173. [PubMed: 17627087]

Edwards DS, Clasper JC, 2015 Heterotopic ossification: a systematic review. J R Army Med Corps 161, 315–321. [PubMed: 25015927]

Ellis GK, Bone HG, Chlebowski R, Paul D, Spadafora S, Smith J, Fan M, Jun S, 2008 Randomized trial of denosumab in patients receiving adjuvant aromatase inhibitors for nonmetastatic breast cancer. J Clin Oncol 26, 4875–4882. [PubMed: 18725648]

Embree M, Ono M, Kilts T, Walker D, Langguth J, Mao J, Bi Y, Barth JL, Young M, 2011 Role of subchondral bone during early-stage experimental TMJ osteoarthritis. J Dent Res 90, 1331–1338. [PubMed: 21917603]

Goldberg M, Septier D, Oldberg A, Young MF, Ameye LG, 2006 Fibromodulin-deficient mice display impaired collagen fibrillogenesis in predentin as well as altered dentin mineralization and enamel formation. J Histochem Cytochem 54, 525–537. [PubMed: 16344330]

Hardingham TE, Fosang AJ, 1992 Proteoglycans: many forms and many functions. FASEB J 6, 861–870. [PubMed: 1740236]

Hildebrand A, Romaris M, Rasmussen LM, Heinegard D, Twardzik DR, Border WA, Ruoslahti E, 1994 Interaction of the small interstitial proteoglycans biglycan, decorin and fibromodulin with transforming growth factor beta. Biochem J 302 (Pt 2), 527–534. [PubMed: 8093006]

Hussar DA, Stevenson T, 2010 New drugs: Denosumab, dienogest/estradiol valerate, and polidocanol. J Am Pharm Assoc (2003) 50, 658–662. [PubMed: 20833626]

Iozzo RV, 1997 The family of the small leucine-rich proteoglycans: key regulators of matrix assembly and cellular growth. Crit Rev Biochem Mol Biol 32, 141–174. [PubMed: 9145286]

Iozzo RV, Murdoch AD, 1996 Proteoglycans of the extracellular environment: clues from the gene and protein side offer novel perspectives in molecular diversity and function. FASEB J 10, 598–614. [PubMed: 8621059]

Iranikhah M, Deas C, Murphy P, Freeman MK, 2018 Effects of Denosumab After Treatment Discontinuation : A Review of the Literature. Consult Pharm 33, 142–151. [PubMed: 29720299]

Jensen LL, Halar E, Little JW, Brooke MM, 1987 Neurogenic heterotopic ossification. Am J Phys Med 66, 351–363. [PubMed: 3124630]

Kalamajski S, Oldberg A, 2010 The role of small leucine-rich proteoglycans in collagen fibrillogenesis. Matrix Biol 29, 248–253. [PubMed: 20080181]

Karasik D, Ferrari SL, 2008 Contribution of gender-specific genetic factors to osteoporosis risk. Ann Hum Genet 72, 696–714. [PubMed: 18485052]

Kim HK, Morgan-Bagley S, Kostenuik P, 2006 RANKL inhibition: a novel strategy to decrease femoral head deformity after ischemic osteonecrosis. J Bone Miner Res 21, 1946–1954. [PubMed: 17002576]

Kohler T, Beyeler M, Webster D, Müller R, 2005 Compartmental bone morphometry in the mouse femur: reproducibility and resolution dependence of microtomographic measurements. Calcif. Tissue Int 77, 281–290. [PubMed: 16283571]

Kostenuik PJ, Nguyen HQ, McCabe J, Warmington KS, Kurahara C, Sun N, Chen C, Li L, Cattley RC, Van G, Scully S, Elliott R, Grisanti M, Morony S, Tan HL, Asuncion F, Li X, Ominsky MS, Stolina M, Dwyer D, Dougall WC, Hawkins N, Boyle WJ, Simonet WS, Sullivan JK, 2009 Denosumab, a fully human monoclonal antibody to RANKL, inhibits bone resorption and increases BMD in knock-in mice that express chimeric (murine/human) RANKL. J Bone Miner Res 24, 182–195. [PubMed: 19016581]

Kram V, Kilts TM, Bhattacharyya N, Li L, Young MF, 2017 Small leucine rich proteoglycans, a novel link to osteoclastogenesis. Sci Rep 7, 12627. [PubMed: 28974711]

Lauder RM, Huckerby TN, Nieduszynski IA, 1995 The structure of the keratan sulphate chains attached to fibromodulin isolated from bovine tracheal cartilage: oligosaccharides generated by keratanase II digestion. Glycoconj J 12, 651–659. [PubMed: 8595256]

Laurent M, Antonio L, Sinnesael M, Dubois V, Gielen E, Classens F, Vanderschueren D, 2014 Androgens and estrogens in skeletal sexual dimorphism. Asian J Androl 16, 213–222. [PubMed: 24385015]

Li X, Pennisi A, Yaccoby S, 2008 Role of decorin in the antimyeloma effects of osteoblasts. Blood 112, 159–168. [PubMed: 18436739]

Locksley RM, Killeen N, Lenardo MJ, 2001 The TNF and TNF receptor superfamilies: integrating mammalian biology. Cell 104, 487–501. [PubMed: 11239407]

Mania VM, Kallivokas AG, Malavaki C, Asimakopoulou AP, Kanakis J, Theocharis AD, Klironomos G, Gatzounis G, Mouzaki A, Panagiotopoulos E, Karamanos NK, 2009 A comparative biochemical analysis of glycosaminoglycans and proteoglycans in human orthotopic and heterotopic bone. IUBMB Life 61, 447–452. [PubMed: 19319964]

McEwan PA, Scott PG, Bishop PN, Bella J, 2006 Structural correlations in the family of small leucine-rich repeat proteins and proteoglycans. J Struct Biol 155, 294–305. [PubMed: 16884925]

Miguez PA, Terajima M, Nagaoka H, Mochida Y, Yamauchi M, 2011 Role of glycosaminoglycans of biglycan in BMP-2 signaling. Biochem Biophys Res Commun 405, 262–266. [PubMed: 21219861]

Miller RE, Branstetter D, Armstrong A, Kennedy B, Jones J, Cowan L, Bussiere J, Dougall WC, 2007 Receptor activator of NF-kappa B ligand inhibition suppresses bone resorption and hypercalcemia but does not affect host immune responses to influenza infection. J Immunol 179, 266–274. [PubMed: 17579046]

Mochida Y, Parisuthiman D, Yamauchi M, 2006 Biglycan is a positive modulator of BMP-2 induced osteoblast differentiation. Adv Exp Med Biol 585, 101–113. [PubMed: 17120779]

Moen MD, Keam SJ, 2011 Denosumab: a review of its use in the treatment of postmenopausal osteoporosis. Drugs Aging 28, 63–82. [PubMed: 21174488]

Ominsky MS, Kostenuik PJ, Cranmer P, Smith SY, Atkinson JE, 2007 The RANKL inhibitor OPG-Fc increases cortical and trabecular bone mass in young gonad-intact cynomolgus monkeys. Osteoporos. Int. 18, 1073–1082.

Ominsky MS, Li X, Asuncion FJ, Barrero M, Warmington KS, Dwyer D, Stolina M, Geng Z, Grisanti M, Tan HL, Corbin T, McCabe J, Simonet WS, Ke HZ, Kostenuik PJ, 2008 RANKL inhibition with osteoprotegerin increases bone strength by improving cortical and trabecular bone architecture in ovariectomized rats. J Bone Miner Res 23, 672–682. [PubMed: 18433301]

Padagas J, Colloton M, Shalhoub V, Kostenuik P, Morony S, Munyakazi L, Guo M, Gianneschi D, Shatzen E, Geng Z, Tan HL, Dunstan C, Lacey D, Martin D, 2006 The receptor activator of nuclear factor-kappaB ligand inhibitor osteoprotegerin is a bone-protective agent in a rat model of chronic renal insufficiency and hyperparathyroidism. Calcif Tissue Int 78, 35–44. [PubMed: 16362459]

Pietschmann P, Rauner M, Sipos W, Kerschan-Schindl K, 2009 Osteoporosis: an age-related and gender-specific disease--a mini-review. Gerontology 55, 3–12. [PubMed: 18948685]

Reid IR, Miller PD, Brown JP, Kendler DL, Fahrleitner-Pammer A, Valter I, Maasalu K, Bolognese MA, Woodson G, Bone H, Ding B, Wagman RB, San Martin J, Ominsky MS, Dempster DW, Denosumab Phase 3 Bone Histology Study, G., 2010 Effects of denosumab on bone histomorphometry: the FREEDOM and STAND studies. J Bone Miner Res 25, 2256–2265. [PubMed: 20533525]

Saamanen AM, Salminen HJ, Rantakokko AJ, Heinegard D, Vuorio EI, 2001 Murine fibromodulin: cDNA and genomic structure, and age-related expression and distribution in the knee joint. Biochem J 355, 577–585. [PubMed: 11311118]

Schaefer L, Iozzo RV, 2008 Biological functions of the small leucine-rich proteoglycans: from genetics to signal transduction. J. Biol. Chem 283, 21305–21309. [PubMed: 18463092]

Shehab D, Elgazzar AH, Collier BD, 2002 Heterotopic ossification. J. Nucl. Med 43, 346–353. [PubMed: 11884494]

Simonet WS, Lacey DL, Dunstan CR, Kelley M, Chang MS, Luthy R, Nguyen HQ, Wooden S, Bennett L, Boone T, Shimamoto G, DeRose M, Elliott R, Colombero A, Tan HL, Trail G, Sullivan J, Davy E, Bucay N, Renshaw-Gegg L, Hughes TM, Hill D, Pattison W, Campbell P, Sander S, Van G, Tarpley J, Derby P, Lee R, Boyle WJ, 1997 Osteoprotegerin: a novel secreted protein involved in the regulation of bone density. Cell 89, 309–319. [PubMed: 9108485]

Sipos W, Zysset P, Kostenuik P, Mayrhofer E, Bogdan C, Rauner M, Stolina M, Dwyer D, Sommerfeld-Stur I, Pendl G, Resch H, Dall'Ara E, Varga P, Pietschmann P, 2011 OPG-Fc treatment in growing pigs leads to rapid reductions in bone resorption markers, serum calcium, and bone formation markers. Horm Metab Res 43, 944–949. [PubMed: 22161252]

Takeuchi Y, Kodama Y, Matsumoto T, 1994 Bone matrix decorin binds transforming growth factor-beta and enhances its bioactivity. J Biol Chem 269, 32634–32638. [PubMed: 7798269]

Theoleyre S, Kwan Tat S, Vusio P, Blanchard F, Gallagher J, Ricard-Blum S, Fortun Y, Padrines M, Redini F, Heymann D, 2006 Characterization of osteoprotegerin binding to glycosaminoglycans by surface plasmon resonance: role in the interactions with receptor activator of nuclear factor kappaB ligand (RANKL) and RANK. Biochem Biophys Res Commun 347, 460–467. [PubMed: 16828054]

Urist MR, Nakagawa M, Nakata N, Nogami H, 1978 Experimental myositis ossificans: cartilage and bone formation in muscle in response to a diffusible bone matrix-derived morphogen. Arch Pathol Lab Med 102, 312–316. [PubMed: 580725]

Waddington RJ, Roberts HC, Sugars RV, Schonherr E, 2003 Differential roles for small leucine-rich proteoglycans in bone formation. Eur Cell Mater 6, 12–21; discussion 21. [PubMed: 14562268]

Wadhwa S, Embree M, Ameye L, Young MF, 2005 Mice deficient in biglycan and fibromodulin as a model for temporomandibular joint osteoarthritis. Cells Tissues Organs 181, 136–143. [PubMed: 16612079]

Wang L, Foster BL, Kram V, Nociti FH Jr., Zerfas PM, Tran AB, Young MF, Somerman MJ, 2014 Fibromodulin and Biglycan Modulate Periodontium through TGFbeta/BMP Signaling. J Dent Res 93, 780–787. [PubMed: 24966230]

Wilkie AOM, Morriss-Kay GM, 2001 Genetics of craniofacial development and malformation. Nature Reviews Genetics 2, 458–468.

Winge SB, Nielsen J, Jorgensen A, Owczarek S, Ewen KA, Nielsen JE, Juul A, Berezin V, Rajpert-De Meyts E, 2015 Biglycan is a novel binding partner of fibroblast growth factor receptor 3c (FGFR3c) in the human testis. Mol Cell Endocrinol 399, 235–243. [PubMed: 25260943]

Xaus J, Comalada M, Cardo M, Valledor AF, Celada A, 2001 Decorin inhibits macrophage colony-stimulating factor proliferation of macrophages and enhances cell survival through induction of p27(Kip1) and p21(Waf1). Blood 98, 2124–2133. [PubMed: 11567999]

Xu T, Bianco P, Fisher LW, Longenecker G, Smith E, Goldstein S, Bonadio J, Boskey A, Heegaard AM, Sommer B, Satomura K, Dominguez P, Zhao C, Kulkarni AB, Robey PG, Young MF, 1998 Targeted disruption of the biglycan gene leads to an osteoporosis-like phenotype in mice. Nat Genet 20, 78–82. [PubMed: 9731537]

Yamaguchi Y, Mann DM, Ruoslahti E, 1990 Negative regulation of transforming growth factor-beta by the proteoglycan decorin. Nature 346, 281–284. [PubMed: 2374594]

Yasuda H, Shima N, Nakagawa N, Mochizuki SI, Yano K, Fujise N, Sato Y, Goto M, Yamaguchi K, Kuriyama M, Kanno T, Murakami A, Tsuda E, Morinaga T, Higashio K, 1998a Identity of osteoclastogenesis inhibitory factor (OCIF) and osteoprotegerin (OPG): a mechanism by which OPG/OCIF inhibits osteoclastogenesis in vitro. Endocrinology 139, 1329–1337. [PubMed: 9492069]

Yasuda H, Shima N, Nakagawa N, Yamaguchi K, Kinosaki M, Mochizuki S, Tomoyasu A, Yano K, Goto M, Murakami A, Tsuda E, Morinaga T, Higashio K, Udagawa N, Takahashi N, Suda T, 1998b Osteoclast differentiation factor is a ligand for osteoprotegerin/osteoclastogenesis-inhibitory factor and is identical to TRANCE/RANKL. Proc Natl Acad Sci U S A 95, 3597–3602. [PubMed: 9520411]

Zanotti S, Kalajzic I, Aguila HL, Canalis E, 2014 Sex and genetic factors determine osteoblastic differentiation potential of murine bone marrow stromal cells. PLoS One 9, e86757. [PubMed: 24489784]

Zotz TG, Paula JB, Moser AD, 2012 Experimental model of heterotopic ossification in Wistar rats. Braz J Med Biol Res 45, 497–501. [PubMed: 22473322]

Highlights:

- *Bgn/Fmod* DKO mice have low bone mass (LBM) and other mineralized tissue defects
- *Bgn/Fmod* DKO and WT were injected with OPG-Fc to rescue and repair LBM
- OPG-Fc treatment in young mice was harmful to the growth of craniofacial and long bones
- Treatment improved some parameters in older DKO mice but was unable to restore them to WT levels
- Treatment was not able to prevent the formation of ectopic ossification in *Bgn/Fmod* DKO mice

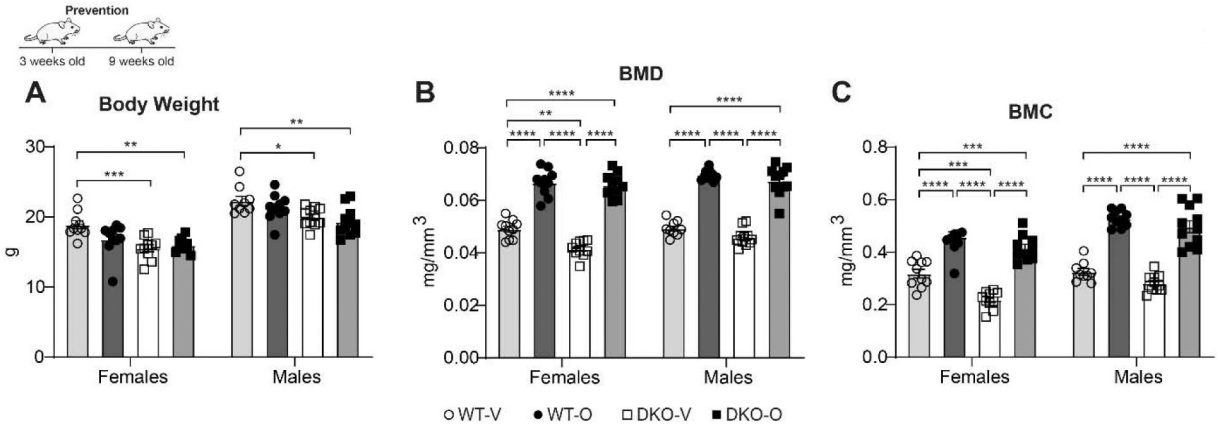

Figure 1:

Impact of OPG-Fc treatment of skeletally immature mice on body weight, BMD and BMC (A.) whole body weight; (B.) BMD and (C.) BMC obtained by DEXA analysis. Data are mean ± SE obtained from N = 10 mice per group. Analyzed by two-way ANOVA and Tukey's post hoc. *, $p<0.05$; **, $p<0.01$; ***, $p<0.001$; ****, $p<0.0001$. WT-V: wild type vehicle treated; WT-O: wild type OPG-Fc treated; DKO-V: *Bgn/Fmod double knockout* vehicle treated; DKO-O: *Bgn/Fmod double knockout* OPG-Fc treated.

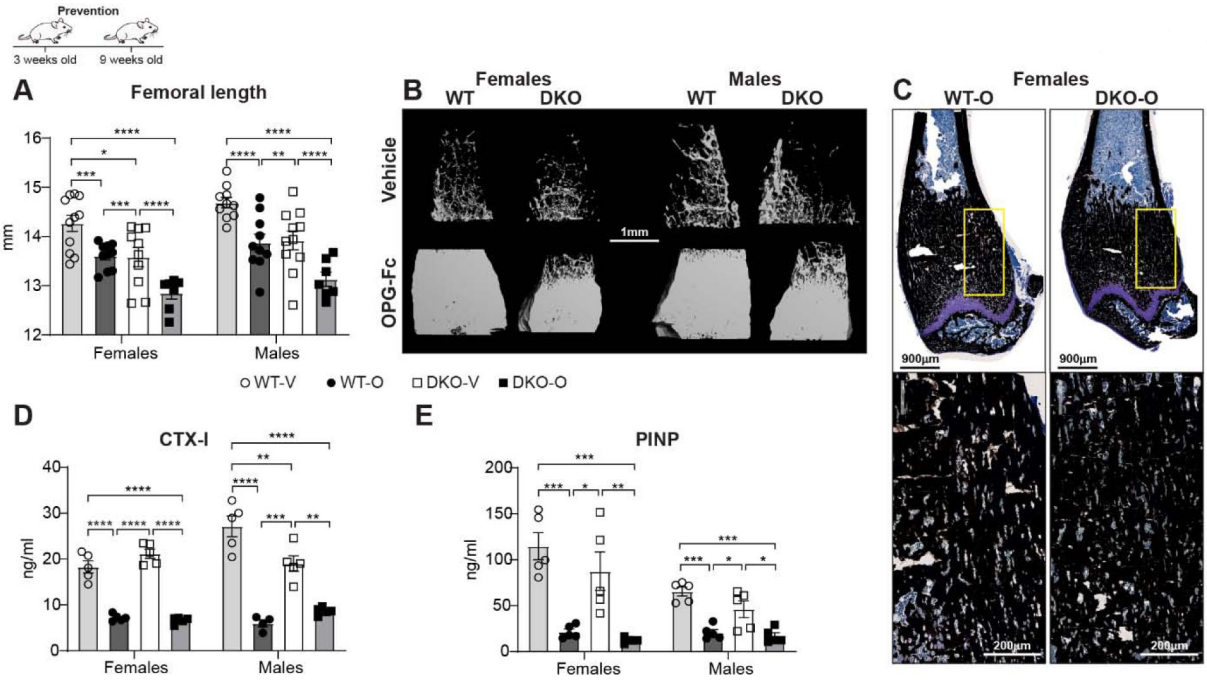

Figure 2:

Adverse effects of OPG-Fc treatment on the skeleton of young mice. (A.) femoral length; (B.) 3D reconstructed µCT images of the femoral metaphysis of OPG-Fc- vs. vehicle-treated WT and *Bgn/Fmod* DKO mice demonstrating a calcified mass filling the trabecular compartment. Data are mean ± SE obtained from N=10 mice per group. Analyzed by two-way ANOVA. *and Tukey's post hoc* *, p<0.05; **, p<0.01; ***, p<0.001. (C.) Von Kossa stained sections of representative femurs demonstrating acellular trabecular compartment with (almost) completely obliterated marrow space. Serum levels of (D.) bone resorption and (E.) bone formation markers. Serum was obtained from 9-weeks old mice before sacrifice and measured using commercial ELISA kits. Data are mean ± SE obtained from N=5. Analyzed by two-way ANOVA *and Tukey's post hoc*. *, p<0.05; **, p<0.01; ***, p<0.001; ****, p<0.0001. WT-V: wild type vehicle treated; WT-O: wild type OPG-Fc treated; DKO-V: *Bgn/Fmod* double knockout vehicle treated; DKO-O: *Bgn/Fmod* double knockout OPG-Fc treated.

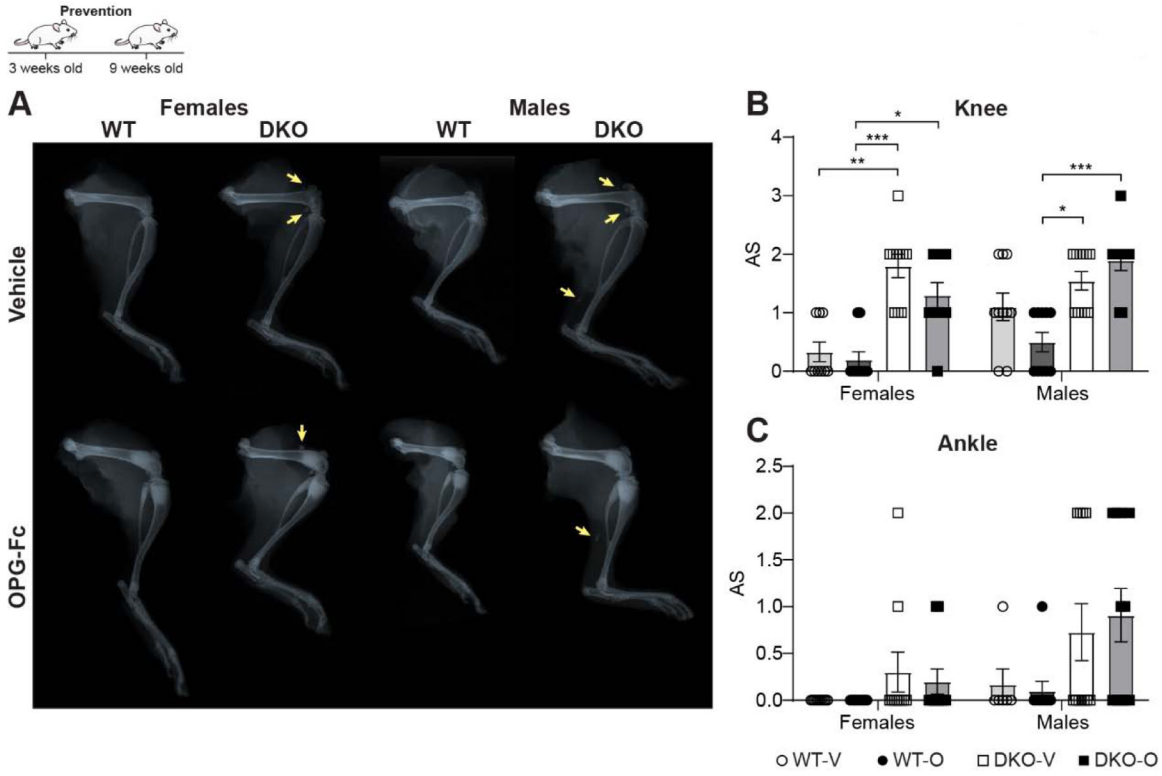

Figure 3:

Effect of OPG-Fc treatment in young mice on ectopic ossification. (A.) x-ray image of hind leg demonstrating EO lesions (marked by yellow arrows) in knee and Achilles ligament of *Bgn/Fmod* DKO mice. Note the massive radio-opaque area in the distal metaphysis of the femur and proximal metaphysis of the tibia in the OPG-Fc treated groups. EO scoring of (B.) Knee and (C.) ankle areas using arbitrary units. Data are mean ± SE obtained from N=7–10. Analyzed by ordinal regression *followed by Dunn's post hoc test*. *, $p<0.05$; **, $p<0.01$; ***, $p<0.001$. WT-V: wild type vehicle treated; WT-O: wild type OPG-Fc treated; DKO-V: *Bgn/Fmod* double knockout vehicle treated; DKO-O: *Bgn/Fmod* double knockout OPG-Fc treated.

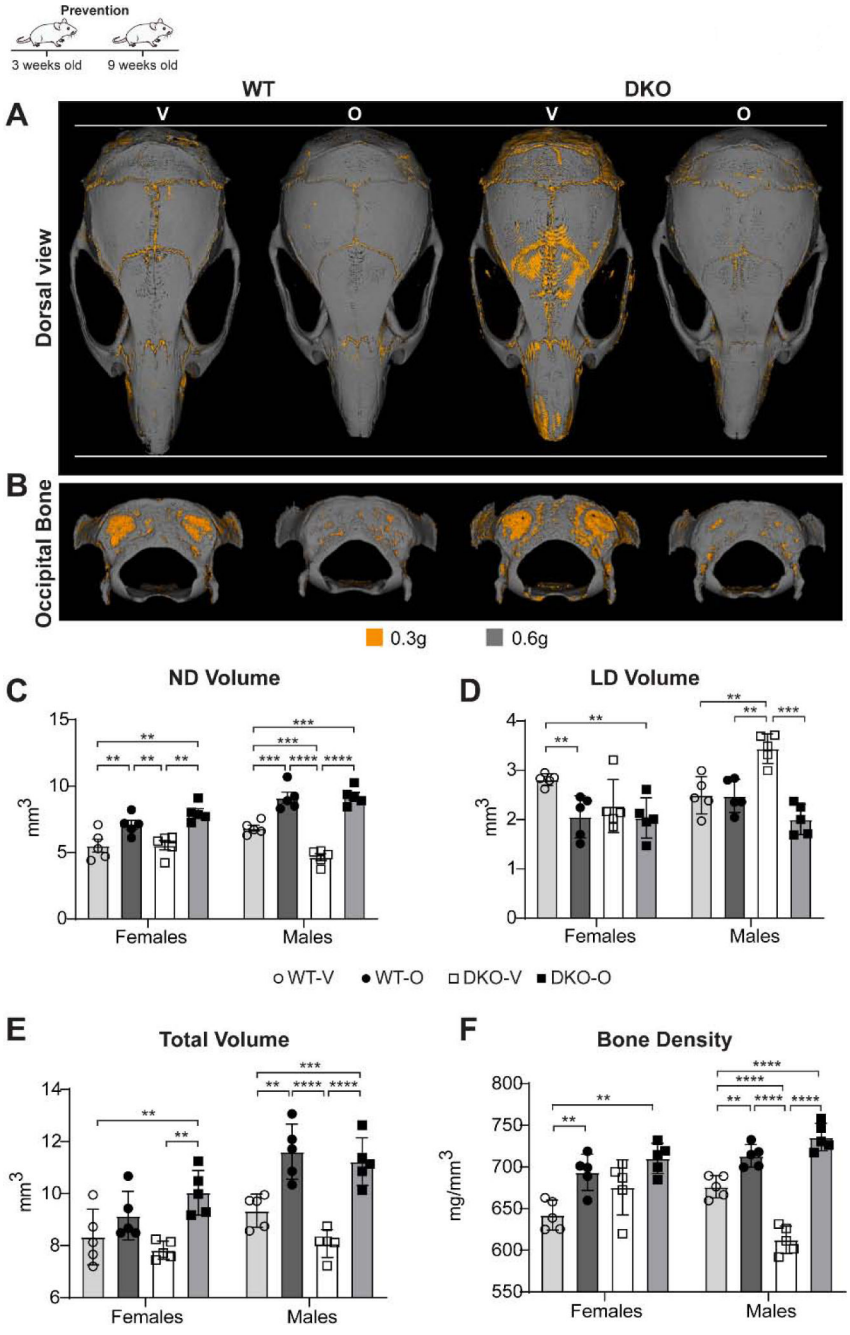

Figure 4:

μCT analysis of craniofacial skeleton of the prevention module. (A.) 3D renderings of 9-week old male skulls (Dorsal view) showing normal density (ND) bone (0.6g HA/cm^3) in gray and low density (LD) bone (0.3–0.59g HA/cm^3) in orange. (B.) Posterior view of skull showing the occipital bone. Quantification of the changes in (C.) ND bone (D.) LD bone volume. (E.) Total volume (TV) and (F.) Bone Density of the occipital bone. Data are mean ± SE obtained from N = 5 mice per group. Analyzed by two-way ANOVA, and Tukey's post-hoc. *, p<0.05; **, p<0.01; ***, p<0.001; ****, p<0.0001. WT-V: wild type vehicle

treated; WT-O: wild type OPG-Fc treated; DKO-V: *Bgn/Fmod* double knockout vehicle treated; DKO-O: *Bgn/Fmod* double knockout OPG-Fc treated.

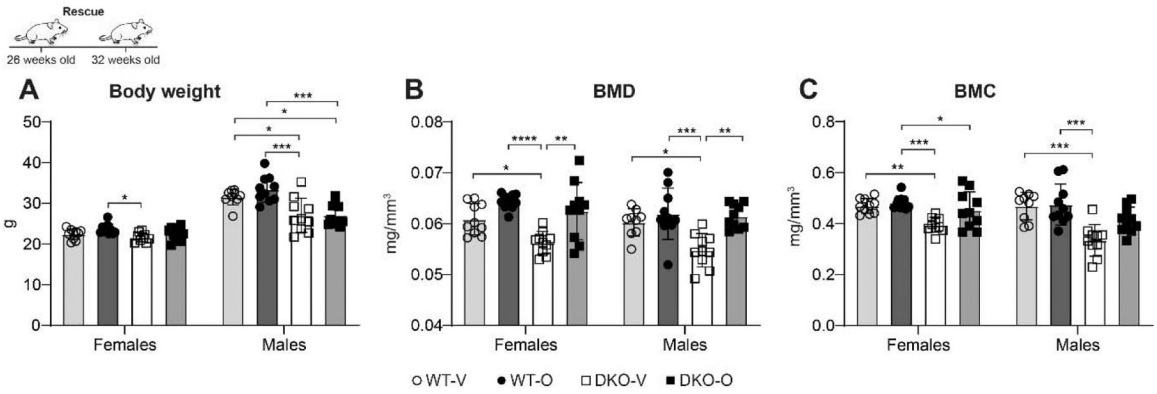

Figure 5:

Impact of OPG-Fc treatment of skeletally mature mice on body weight, BMD and BMC (A.) whole body weight; (B.) BMD and (C.) BMC obtained by DEXA analysis. Data are mean ± SE obtained from N = 10 mice per group. Analyzed by two-way ANOVA *and Tukey's post hoc*. *, p<0.05; **, p<0.01; ***, p<0.001*; ****, p<0.0001*. WT-V: wild type vehicle treated; WT-O: wild type OPG-Fc treated; DKO-V: *Bgn/Fmod* double knockout vehicle treated; DKO-O: *Bgn/Fmod* double knockout OPG-Fc treated.

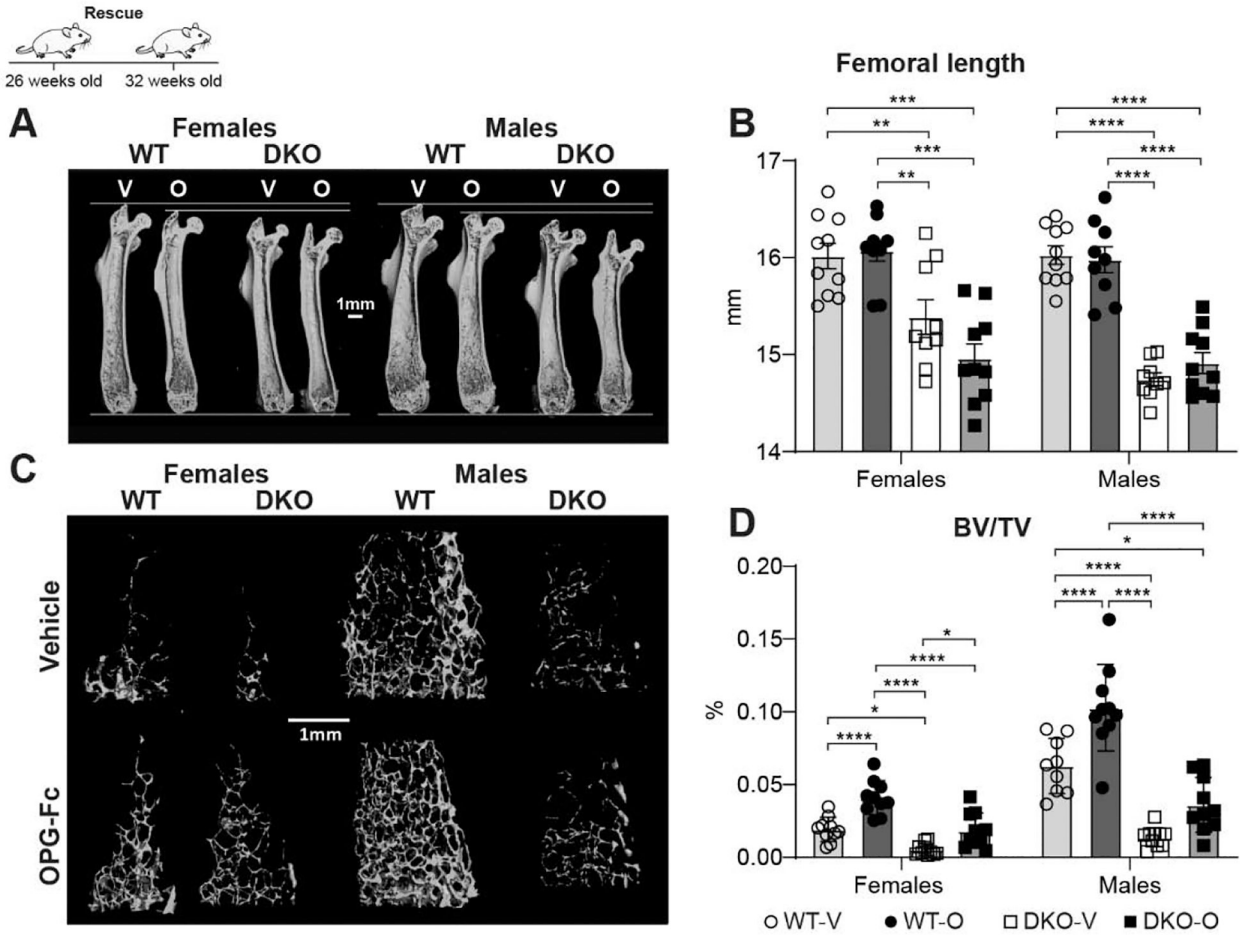

Figure 6:

Impact of OPG-Fc treatment in mature mice on longitudinal growth and trabecular bone microarchitecture. (A.) 3D rendering of μCT femoral scans from 32w old WT and *Bgn/Fmod* DKO mice; (B.) femoral length; (C.) 3D rendering of distal femoral metaphyseal bone. Images from each group were obtained from animals with median metaphyseal trabecular bone density values. (D.) Quantitative μCT analysis of Trabecular bone volume density (BV/TV). Data are mean ± SE obtained from N = 10 mice per group *, $p<0.05$; **, $p<0.01$; ***, $p<0.001$; ****, $p<0.0001$ by two-way ANOVA and Tukey's post hoc. WT-V: wild type vehicle treated; WT-O: wild type OPG-Fc treated; DKO-V: *Bgn/Fmod* double knockout vehicle treated; DKO-O: *Bgn/Fmod* double knockout OPG-Fc treated.

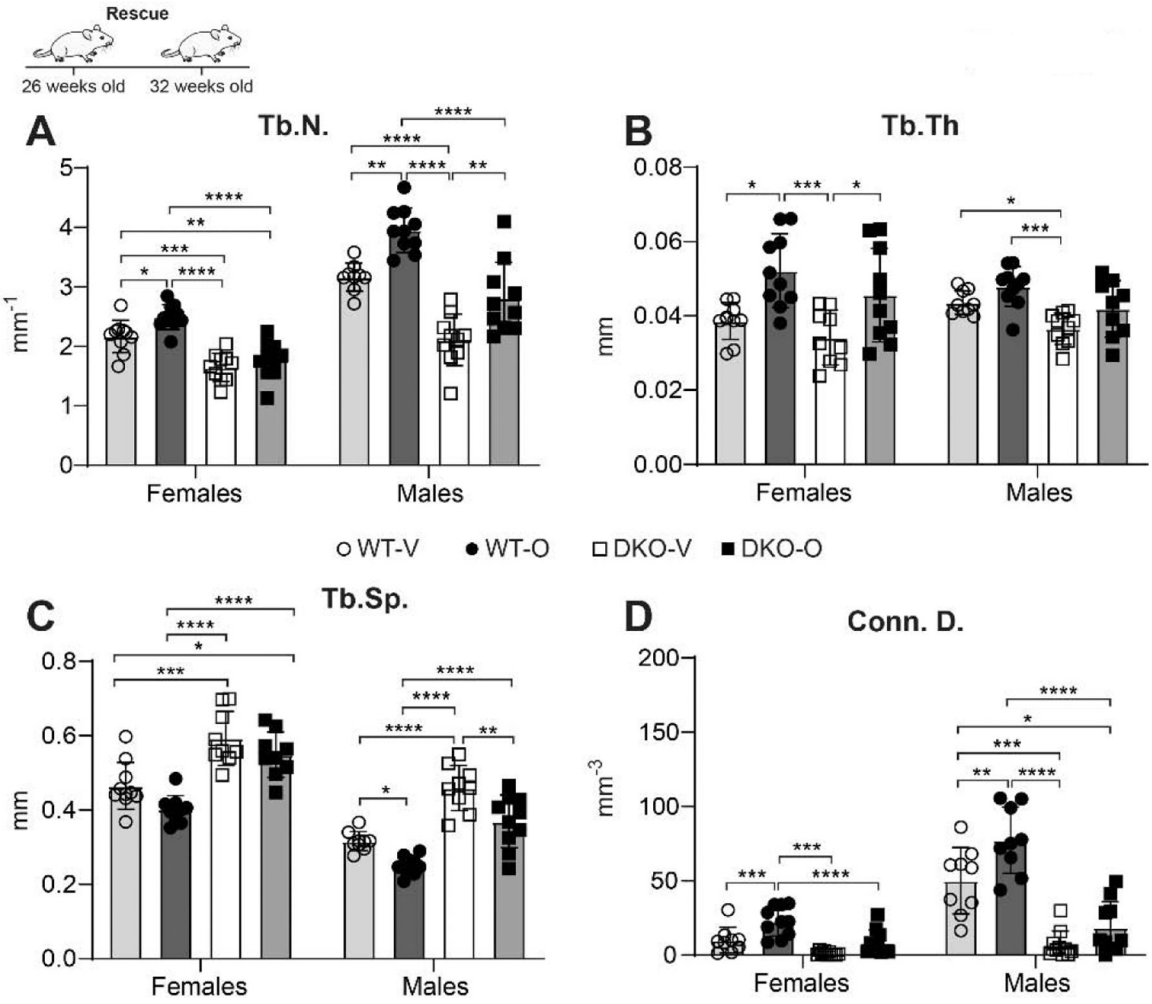

Figure 7:

Trabecular parameters of OPG-Fc and Vehicle-treated WT and *Bgn/Fmod* DKO mice at the end of the repair module (32 weeks). Quantitative μCT analysis of: (A.) Trabecular number (Tb.N.); (B) Trabecular thickness (Tb.Th.); (C.) Trabecular spacing (Tb.Sp.); (D.) Connectivity Density (Conn. D.). Data are mean ± SE obtained from N = 10 mice per group. *, $p < 0.05$; **, $p < 0.01$; ***, $p < 0.001$; ****, $p<0.0001$. Analyzed by two-way ANOVA *with Tukey's post hoc*. WT-V: wild type vehicle treated; WT-O: wild type OPG-Fc treated; DKO-V: *Bgn/Fmod* double knockout vehicle treated; DKO-O: *Bgn/Fmod* double knockout OPG-Fc treated.

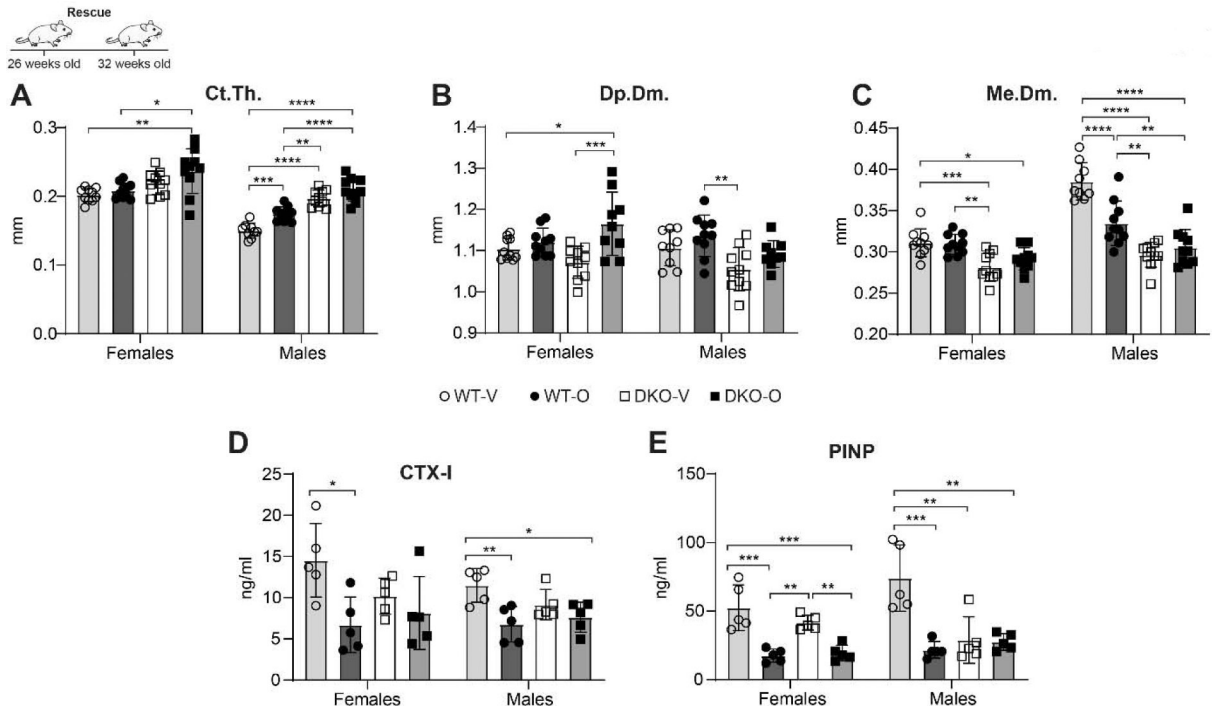

Figure 8:

Cortical dimensions and serum markers of OPG-Fc and Vehicle-treated WT and *Bgn/Fmod* DKO mice at end of the repair module (32 weeks). Quantitative μCT analysis of: (A.) mid-diaphyseal cortical thickness (Ct.Th.); (B.) mid-diaphyseal diameter (Dp.Dm.); (C.) medullary cavity diameter (Me.Dm). Data are mean ± SE obtained from N = 10 mice per group. Analyzed by two-way ANOVA *and Tukey's post hoc* *, $p < 0.05$; **, $p < 0.01$; ***, $p < 0.001$; ****, $p < 0.0001$. Serum levels of (D.) bone resorption and (E.) bone formation markers. Serum was obtained from 32-weeks old mice before sacrifice and measured using commercial ELISA kits. Data are mean ± SE obtained from N=5. Analyzed by two-way ANOVA *and Tukey's post hoc*. *, $p<0.05$; **, $p<0.01$; ***, $p<0.001$; ****, $p<0.0001$. WT-V: wild type vehicle treated; WT-O: wild type OPG-Fc treated; DKO-V: *Bgn/Fmod* double knockout vehicle treated; DKO-O: *Bgn/Fmod* double knockout OPG-Fc treated.

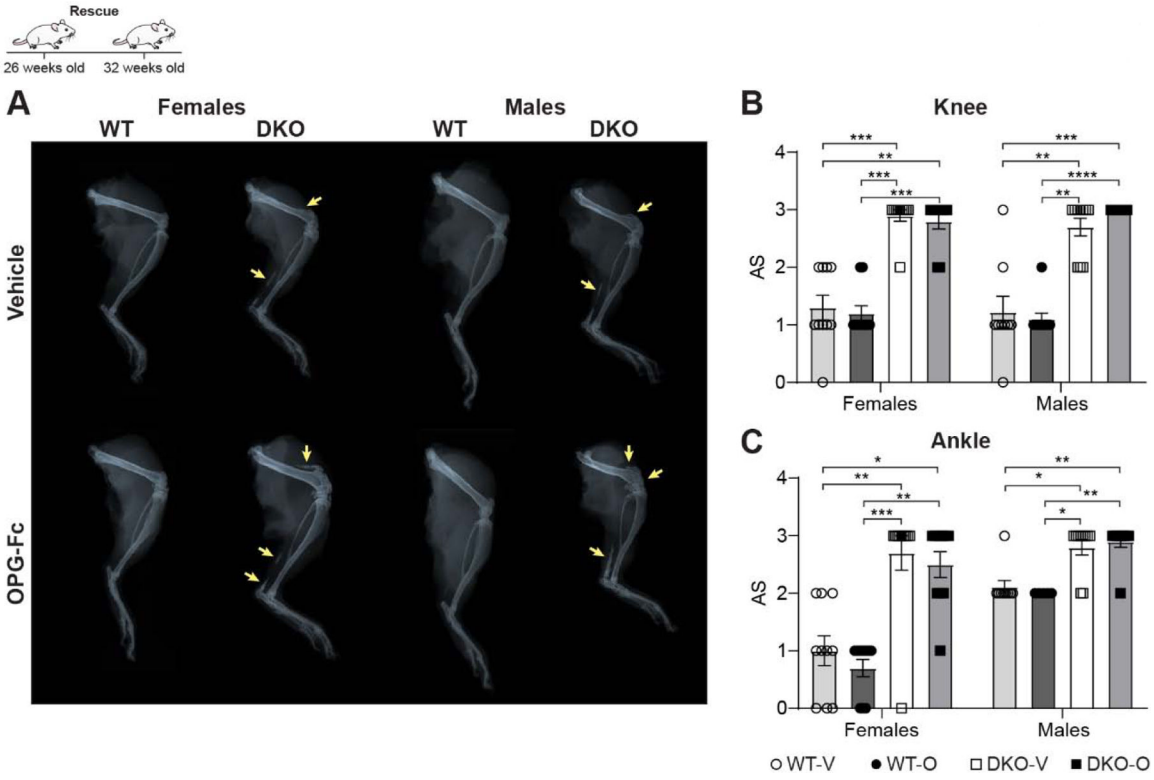

Figure 9: Effect of OPG-Fc treatment in mature mice on ectopic ossification.

(A.) x-ray image of hind leg demonstrating more and bigger EO lesions (marked by yellow arrows) in knee and Achilles ligament of both OPG-Fc- and vehicle-treated *Bgn/Fmod* DKO and WT mice. EO scoring of (B.) Knee and (C.) ankle areas using arbitrary units. Data are mean ± SE obtained from N=7–10. Analyzed by ordinal regression. *, $p<0.05$; **, $p<0.01$; ***, $p<0.001$; ****, $p<0.0001$. WT-V: wild type vehicle treated; WT-O: wild type OPG-Fc treated; DKO-V: *Bgn/Fmod* double knockout vehicle treated; DKO-O: *Bgn/Fmod* double knockout OPG-Fc treated.

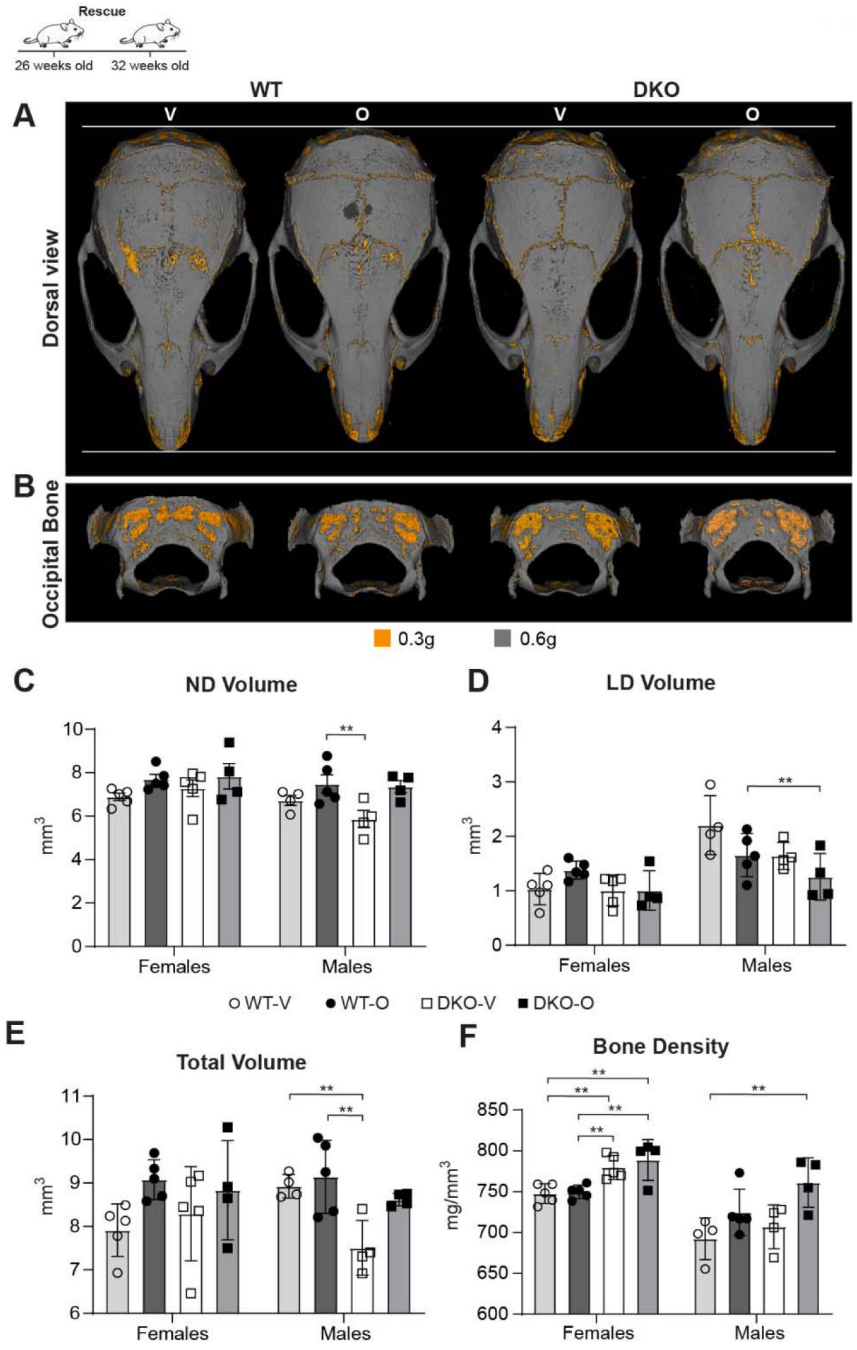

Figure 10:

μCT analysis of craniofacial skeleton of rescue module. (A.) 3D rendering of 32-week-old male skulls (Dorsal view). ND bone (0.6g HA/cm^3) is gray whereas LD bone (0.3–0.59g HA/cm^3) is orange. (B.) Posterior view of the same skulls showing occipital bone. Quantification of changes in (C.) ND (D.) LD volume (E.) Total volume (TV) and (F.) Bone density of the occipital bone. Data are mean ± SE analyzed by two-way ANOVA and Tukey's post-hoc Data are mean ± SE analyzed by two-way ANOVA, obtained from N = 5 mice per group *, p<0.05; **, p<0.01; ***, p<0.001; ****, p<0.0001. WT-V: wild type

vehicle treated; WT-O: wild type OPG-Fc treated; DKO-V: *Bgn/Fmod* double knockout vehicle treated; DKO-O: Bgn/Fmod double knockout OPG-Fc treated.